All-organic thermally activated delayed fluorescence materials for organic light-emitting diodes

Yuchao Liu[1,3], Chensen Li[1,3], Zhongjie Ren[1], Shouke Yan[1]* and Martin R. Bryce[2]**

Abstract | Thermally activated delayed fluorescence (TADF) emitters, which produce light by harvesting both singlet and triplet excitons without noble metals, are emerging as next-generation organic electroluminescent materials. In the past few years, there have been rapid advances in molecular design criteria, our understanding of the photophysics underlying TADF and the applications of TADF materials as emitters in organic light-emitting diodes (OLEDs). This topic is set to remain at the forefront of research in optoelectronic organic materials for the foreseeable future. In this Review, we focus on state-of-the-art materials design and understanding of the photophysical processes, which are being leveraged to optimize the performance of OLED devices. Notably, we also appraise dendritic and polymeric TADF emitters — macromolecular materials that offer the potential advantages of low cost, solution processable and large-area OLED fabrication.

Organic light-emitting diodes (OLEDs) are important for display and illumination technologies owing to their high efficiency, flexible device structures and multicolour emission[1,2]. However, conventional fluorescent OLEDs suffer from an internal quantum efficiency (IQE) of 25% as a consequence of spin statistics, and phosphorescent OLEDs use rare noble metals (for example, Ir and Pt)[3–5]. To overcome these drawbacks, noble metal-free, thermally activated delayed fluorescence (TADF) OLEDs are emerging as next-generation devices[6–8]. TADF OLEDs are likely to be used in display and illumination technologies as well as fluorescence microscopy and sensing applications.

In this Review, we describe the mechanism of TADF and detail the progress that has been made in improving the efficiencies of all-organic TADF-based OLEDs. We also highlight advances in the molecular design and photophysical characteristics of the three classes of organic TADF emitters — organic small molecules, dendrimers and polymers — and OLEDs based on these molecules.

TADF mechanism

During the electroluminescence of TADF emitters (FIG. 1), singlet and triplet states are generated by combining holes and electrons through electrostatic binding. The singlet excitons can decay radiatively with prompt fluorescence (PF), decay nonradiatively or transform into triplet excitons by intersystem crossing (ISC). Simultaneously, low-energy triplet excitons decay nonradiatively or up-convert to the emissive singlet level by an endothermic reverse ISC (RISC) process with delayed fluorescence (DF). Thus, by harvesting both singlet and triplet excitons, an IQE of nearly 100% can be achieved.

To utilize singlet and triplet excitons simultaneously and maximize the IQE, the energy transition processes for TADF emitters must be optimized. As shown in the Arrhenius equation (equation 1), the RISC rate constant k^T_{RISC} from triplet to singlet is closely related to the singlet–triplet energy splitting (ΔE_{ST}), which is defined as the gap between the lowest energy triplet (T_1) and singlet (S_1) excited states:

$$k^T_{RISC} \propto \exp\left(-\Delta E_{ST}/k_B T\right)$$

in which k_B is the Boltzmann constant and T is the temperature.

Enhanced spin–orbit coupling (SOC) between singlet and triplet states can simultaneously lead to relatively high rates of the ISC process and the endothermic reverse process[9]. The RISC rate constant can also be computed in the framework of Fermi's golden rule, which is related to the SOC matrix elements[10,11].

A small ΔE_{ST} is the most important criterion for achieving high TADF efficiency. A small ΔE_{ST} will boost up-conversion from triplet to singlet states and potentially increase the IQE of a device. It is generally recognized that $\Delta E_{ST} < 0.2$ eV is favourable for an efficient RISC process[6]. Higher temperatures provide sufficient

[1]*Beijing Advanced Innovation Center for Soft Matter Science and Engineering, State Key Laboratory of Chemical Resource Engineering, Beijing University of Chemical Technology, Beijing, China.*

[2]*Department of Chemistry, Durham University, Durham, UK.*

[3]*These authors contributed equally: Yuchao Liu, Chensen Li*

**e-mail: renzj@mail.buct.edu.cn; skyan@mail.buct.edu.cn; m.r.bryce@durham.ac.uk*

doi:10.1038/natrevmats.2018.20
Published online 10 Apr 2018

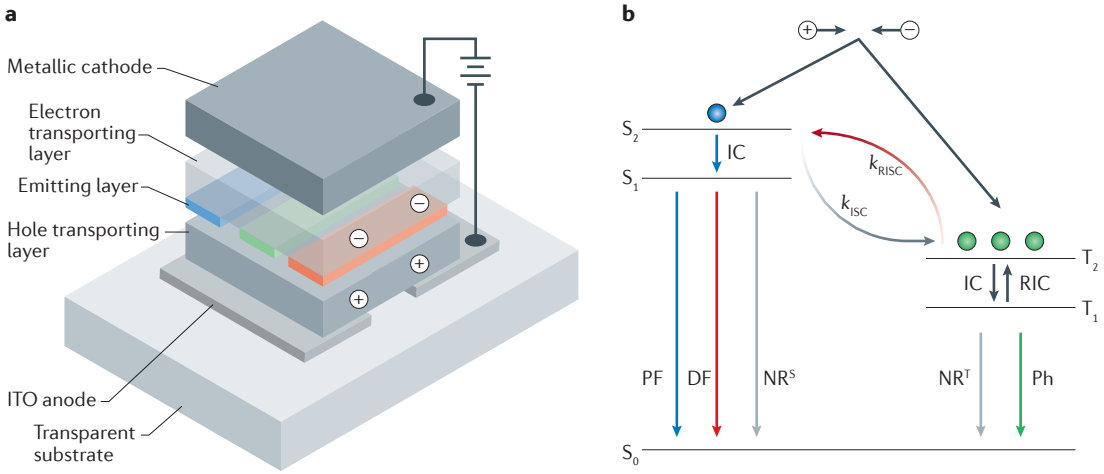

Figure 1 | **Mechanism of TADF OLEDs. a** | The multilayer architecture of thermally activated delayed fluorescence (TADF) organic light-emitting diodes (OLEDs) including a metallic cathode, electron-transport layer, emitting layer, hole-transport layer and indium tin oxide (ITO) anode. Upon application of an electrical field, OLEDs convert electricity into light. **b** | The TADF mechanism that occurs during electroluminescence: singlet and triplet excitons are formed after electron–hole recombination in a singlet:triplet ratio of 1:3. The high exciton states are transferred to the lowest exciton states (S_1 or T_1) via internal conversion (IC), and the accumulated triplet excitons at T_1 are transferred back to S_1 via a reverse intersystem crossing (RISC) process with the aid of thermal activation. The singlet excitons at S_1 formed either initially after electronic excitation or back-transfer from T_1 are radiatively deactivated to S_0 following a prompt fluorescence (PF) decay mechanism for fluorescent emissions with different luminescence lifetimes of PF and delayed fluorescence (DF) decay or non-radiative (NR) decay. In addition, T_1 states are radiatively deactivated to S_0 following a phosphorescence (Ph) decay mechanism for phosphorescent emissions or NR decay. ISC, intersystem crossing; k_{ISC}, rate constant of ISC; k_{RISC}, rate constant of endothermic RISC; NR^S, singlet nonradiative decay; NR^T, triplet nonradiative decay; RIC, reverse internal conversion.

energy to overcome the barrier to RISC. Moreover, a small ΔE_{ST} can be accomplished only by minimizing the electron–electron repulsion of the triplet state[12–14]. From a molecular viewpoint, a spatially twisted structure usually enables a small ΔE_{ST}, because the effective separation of the highest occupied molecular orbital (HOMO) and the lowest unoccupied molecular orbital (LUMO) signifies a small exchange integral (J). The relationship between J and ΔE_{ST} can be quantified using equation 2, in which ΔE_{ST} is approximately twice the value of J between the spatial wavefunctions of the HOMO and LUMO[15]:

$$\Delta E_{ST} = E_S - E_T \approx 2J$$

The effects of SOC are generally treated as a perturbation of the exciton transition process. The effects can be enhanced by the nature of the excited states. In general, the charge-transfer (CT) state is predominant in the singlet excited state. Therefore, to achieve SOC and efficient thermally activated RISC, the triplet excited states on the donor or acceptor units should possess predominant local triplet excited state (^{3}LE) character. If this occurs, one or both of the local triplets on the donor or acceptor units can be in near-resonance with the predominant singlet CT state (^{1}CT). This situation is consistent with the El-Sayed rule for ISC rates[16,17]. CT emission is coupled with large transition dipoles but low oscillator strength, whereas local excited (LE) emission is coupled with small transition dipoles and large oscillator strength. Therefore, the proportion of CT or LE can be controlled by the molecular structure. However, if the excited states have hybrid LE and CT states[18,19] or if the singlet excited states are approximately equal to the corresponding triplet states[20], relatively weak SOC is obtained. In some cases, the TADF efficiency is enhanced by lone-pair orbitals on heteroatoms (for example, nitrogen and sulfur), which provide a $^3n\pi^*$ triplet state that can mediate the ISC process[21].

Molecular rigidity is another important factor that affects the TADF efficiency. Different conformations of a molecule can yield different TADF efficiencies, which means that flexible donors or acceptors should be avoided[22,23]. For TADF molecules, molecular rigidity is achieved by a large dihedral angle (θ) in a twisted donor–acceptor bipolar structure, caused by bulky substituents or a spiro-junction; all these features are favourable for the RISC process[6–8,24–26].

Increasing the radiative decay rate (k_R) from S_1 to S_0 ensures high luminescence efficiency. A high k_R requires the oscillator strength and the transition dipole moment to be balanced. However, k_R tends to be suppressed by a twisted structure with reduced conjugation. Therefore, it is necessary to reduce the overlap of the HOMO and LUMO orbitals while increasing the rate of decay[24,27–30]. Separating donor and acceptor moieties by a phenyl linker is an established approach to realize high efficiency for TADF emitters. Moreover, a wide and delocalized HOMO distribution is favourable for increasing the k_R of TADF emitters[31].

Compared with conventional fluorescent emitters, which have small full width at half maximum, TADF emitters usually display relatively poor monochromaticity

because the broadened emission spectrum originates from a singlet excited state with strong CT character. A successful approach to improving the emission purity is to suppress molecular rotation between the donor and acceptor moieties[32] by introducing large steric hindrance to the core of the TADF emitter[33] or to increase the rigidity of the acceptor moiety[34].

Good thermal and photochemical stabilities of TADF emitters are important for their application. Stability can be judged by bond dissociation energies under positive or negative polarons. More specifically, the combination of stable acceptor (for example, triazine) and donor units (for example, carbazole), which have relatively high bond dissociation energies, favours TADF devices with long lifetimes[6,31,35–37].

In a device, the external quantum efficiency (EQE or η_{ext}) is the key parameter. As shown in equation 3, the contribution from TADF to the EQE is almost twice that from PF, indicating highly efficient T_1/S_1 up-conversion and that a high proportion of DF is responsible for a high EQE value:

$$\eta_{ext} = [0.25\Phi_p + \{0.75 + 0.25(1-\Phi_p)\}\ \Phi_d/1-\Phi_p\ ]\gamma\eta_{out}$$

in which γ is a charge recombination factor, η_{out} is the light out-coupling efficiency and Φ_p and Φ_d are the photoluminescence quantum yield (PLQY) of the prompt and delayed components, respectively.

The pre-coefficients of 0.25 and 0.75 are the branching ratios of singlet exciton and triplet exciton formation, respectively. The value of η_{out} can be increased by preferential molecular orientation along the horizontal plane of the dipoles of the emitting molecules in the OLED. Higher horizontal dipole ratios improve the efficiency of TADF OLEDs. The lifetime of DF (τ_{DF}) is another key factor for the EQE: a short τ_{DF} is desirable to reduce device efficiency roll-off, which is caused by triplet–triplet annihilation, singlet–triplet annihilation and/or triplet–polaron annihilation[24].

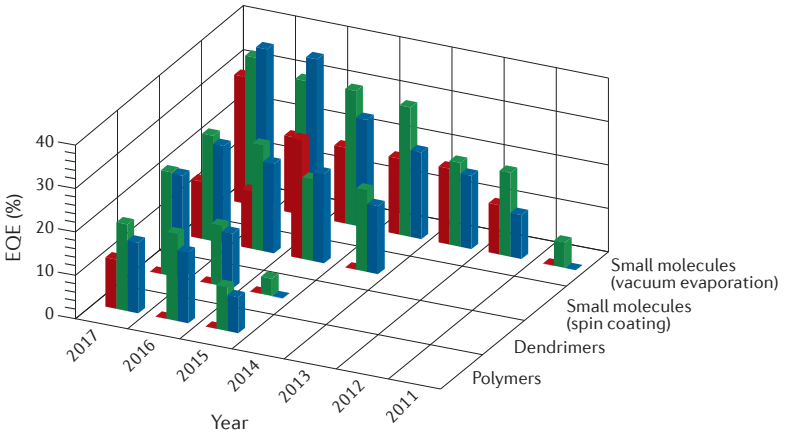

Figure 2 | **External quantum efficiencies of TADF emitters.** Maximum external quantum efficiencies (EQEs) of thermally activated delayed fluorescence (TADF) emitters with red, green and blue emission colours. The data are taken from literature published before the end of December 2017 (Web of Science search).

Efficiency of TADF materials

TADF, initially named E-type delayed fluorescence, was first reported in 1961 in a study on eosin[38]. In 2009, Adachi's group reported SnF_2–porphyrin complexes with TADF properties and OLEDs based on these TADF complexes[39]. The DF of SnF_2–porphyrin complexes is dependent on the temperature, increasing from 0.6% of the total emission at 300 K to 2.4% at 400 K (REF.[39]). Among organometallic TADF-emitting materials, Cu(I) complexes are widely used because of their low cost, facile synthesis and potential for wet fabrication[40,41]. The highly efficient luminescence of Cu(I) compounds with the formula Cu_2X_2(NP) and with Φ_{PL} = 92% has been reported[42], and for dinuclear Cu(I) complexes, NHetPHOS-Cu(I), a maximum EQE (EQE_{max}) of 23% has been obtained. This EQE value is the highest reported for OLEDs with a solution-processed emitting layer based on Cu(I) emitters and is comparable to the efficiency of state-of-the-art thermally evaporated devices based on Ir(III) emitters[43]. The structures of these traditional TADF emitters are shown in Supplementary Figure S1.

Recently, organic molecules have emerged as a class of TADF emitter, providing flexible molecular design, good morphological and electrochemical stabilities and well-controlled photophysical characteristics[7,44]. In the remainder of this Review, we focus on organic TADF emitters, of which there are three distinct classes: small molecules, dendrimers and polymers. The structures of these compounds are shown in Supplementary Figures S2–S6.

The EQEs of OLEDs based on TADF organic small molecules, dendrimers and polymers are improving steadily (FIG. 2). In 2011, Adachi's group[25] reported the first purely aromatic compound, PIC-TRZ, with highly efficient TADF characteristics and a device EQE_{max} of 5.3% at low current density. With the rational choice of molecules with a twisted electron donor–acceptor structure and a high radiative decay rate, highly efficient TADF emitters with a wide range of emission colours have been reported. For example, 4CzIPN (REF.[6]), the structure of which is shown in FIG. 3, exhibits green emission in a doped TADF device with an EQE_{max} of 29.7% at 1,000 cd m^{-2} (REFS[45–47]). Moreover, optimization of the molecular structure and device architecture has resulted in the small-molecule red TADF emitter HAP-3TPA achieving an EQE_{max} of 17.5 ± 1.3% and a peak luminance of 17,000 ± 1,600 cd m^{-2}, despite the inherently low PLQY for red emitters[28]. Combining rigid electron donor and acceptor components gives the orange–red TADF emitters NAI-DMAC and NAI-DPAC, which have record EQEs of 21–29.2% for orange to red TADF OLEDs[48]. The sky-blue TADF emitter spiroAC-TRZ also exhibits excellent device performance, with an EQE_{max} of 36.7% (REF.[29]).

Small molecules are usually dopants within host materials, which can lead to phase separation and poor morphological stability of the emitting layer. Therefore, TADF dendrimers and polymers are attractive alternatives to small-molecule emitters because these macromolecular TADF materials do not require a host material and can be sufficiently soluble in organic solvents to produce thin films by solution processing techniques. For

example, the dendritic TADF emitter **D4** (Supplementary Figure S5) exhibits an EQE_{max} of 13.8%, which remains as high as 13.3% at the high luminance of 1,000 cd m^{-2} in a green device[49], while the polymeric TADF emitter **P8** (Supplementary Figure S6) displays an EQE_{max} of 20.1% in a yellow device[50].

Narrow emission bands with high colour purity are desirable for display applications[24,33,51]. Recently, polycyclic aromatic backbone structures DABNA-1 and DABNA-2 have shown pure blue emission with a full width at half maximum of less than 30 nm, which is much narrower than the typical values of 70–100 nm found for the majority of emitters[32]. However, the full width at half maximum of most macromolecules is still broader than 100 nm. It is noteworthy that a device based on a TADF dendrimer with encapsulated hosts and guests exhibits improved colour purity with a full width at half maximum of nearly 70 nm and Commission Internationale de l'Éclairage (CIE) coordinates of (0.15, 0.30) owing to the reduced host–host and host–guest intermolecular interactions[51]. The design strategy of encapsulating the host and guest separately provides an alternative method to gain solution-processed macromolecular emitters with narrow emission[52].

The operating lifetime of TADF OLEDs is comparable to traditional OLEDs and is continually improving. For example, the lifetime of green OLEDs using the emitter 4CzIPN is 1,380 hours at 1,000 cd m^{-2} after insertion of ultrathin 8-hydroxyquinolatolithium interlayers, which can reduce the number of charge traps and reduce exciton–polaron annihilation; this is comparable to the lifetimes of well-established phosphorescence-based OLEDs[53,54]. Furthermore, the predicted half-life of 10,934 hours for an initial brightness of 1,000 cd m^{-2} can be achieved using 4CzIPN as a green emitter and SF3-TRZ as an n-type host. Compared with p-type hosts, n-type hosts are more suitable for achieving stable electroluminescent devices owing to their inherent ability to balance charge fluxes and suppress high-energy exciton formation[35].

Organic small-molecule TADF materials

Organic small-molecule TADF materials have the benefits of precise molecular structures, high purity (achieved by recrystallization and vacuum sublimation), versatile chemical modification and high luminescence efficiency[55]. The small molecules typically have intramolecular donor–acceptor-type structures incorporating steric hindrance or a twisted conformation, which enhances the CT contribution to the S_1 state (FIG. 3). Various acceptors and donors have been used to tune the TADF characteristics[31], namely, ΔE_{ST}, emission colour, excited state lifetime and TADF quantum yield. The structures of the materials covered in this section are shown in Supplementary Figures S2–S4, and TABLE 1 provides some of their photoluminescence and electroluminescence performances.

Structures and photophysical features

Emission colour. For the realization of full-colour TADF OLEDs, it is vital to systematically modulate the HOMO–LUMO gap and emission colours using suitable donor–acceptor combinations. It is a challenge to prepare blue TADF emitters owing to the required high energies of the CT singlet and triplet states. In this regard, studies on traditional fluorescent materials have shown that limiting the conjugation length[56] and choosing the correct donor units are important to avoid redshifts and to maintain a high triplet level[57]. For blue TADF emitters, donors such as carbazole, diphenylamine, 9,9-dimethyl-9,10-dihydroacridine[31] and their derivatives are commonly used, owing to their moderately strong electron-donating ability and high-energy triplet states, in combination with acceptors with shallow LUMOs that exhibit weak electron-accepting ability[55]. This donor–acceptor pairing ensures that the CT emission is not shifted to lower energy. A typical series of blue TADF emitters are based on a diphenylsulfone acceptor with either diphenylamine, bis(4-tert-butylphenyl)amine or 3,6-di-tert-butylcarbazole donors[8], and their λ_{max} in DPEPO films are 421, 430 and 423 nm, respectively. Among efficient blue TADF molecules, Adachi's group[26] reported a device based on DMAC-DPS (FIG. 3) with a maximum electroluminescence at ~464 nm. A sky-blue OLED based on a DMAC-TRZ emitter (FIG. 3) gave an EQE_{max} of 26.5% and a λ_{max} of ~490 nm (REF.[30]).

Most green TADF emitters incorporate strong electron donors, such as phenoxazine, phenothiazine and dihydrophenazine, as well as highly conjugated carbazole and diphenylamine derivatives[31], and acceptors such as cyano-substituted aromatics, triazine and benzophenone. However, diphenylsulfone and pyrimidine acceptors are less suitable because of their very weak electron-accepting ability. The majority of green to yellow TADF emitters contain cyano-based acceptors. For example, the highly efficient TADF molecule 4CzIPN (FIG. 3) has intense green emission in toluene with a λ_{max} of 507 nm (REF.[6]). Numerous green TADF emitters contain triazine as the acceptor. PXZ-TRZ (FIG. 3) displays green emission with a λ_{max} of 529 nm (REF.[58]). A close analogue gives state-of-the-art green OLEDs ($\lambda_{max} \approx 520$ nm) with an impressive EQE_{max} of 29.6%[59], originating from the optimized oscillator strength and ΔE_{ST}.

Compared with green emitters, relatively few red TADF emitters have been reported. To increase conjugation length, an additional phenyl linker between the donor and acceptor serves to reduce the twist angle between the donor and acceptor[24], thereby giving better orbital overlap and lower-energy emission. However, these features are likely to reduce the efficiency of the RISC process. Orange–red emitters are generally based on dicyanodiazatriphenylene, heptaazaphenalene and anthracenedione acceptors owing to their strong electron-accepting ability with deeper LUMOs[31]. OLEDs prepared with the first near-IR TADF emitter TPA-DCPP (FIG. 3) exhibited an EQE_{max} of 9.8% at a λ_{max} of 645 nm (REF.[19]). Furthermore, an orange–red emitter demonstrated an EQE_{max} of 17.5% owing to efficient up-conversion from T_1 to S_1 (REF.[28]). Two series of anthraquinone-based orange-to-red emitters with CIE coordinates of (0.61, 0.39) and (0.63, 0.37) were also developed, and the highest EQE_{max} among these emitters was 12.5%[24].

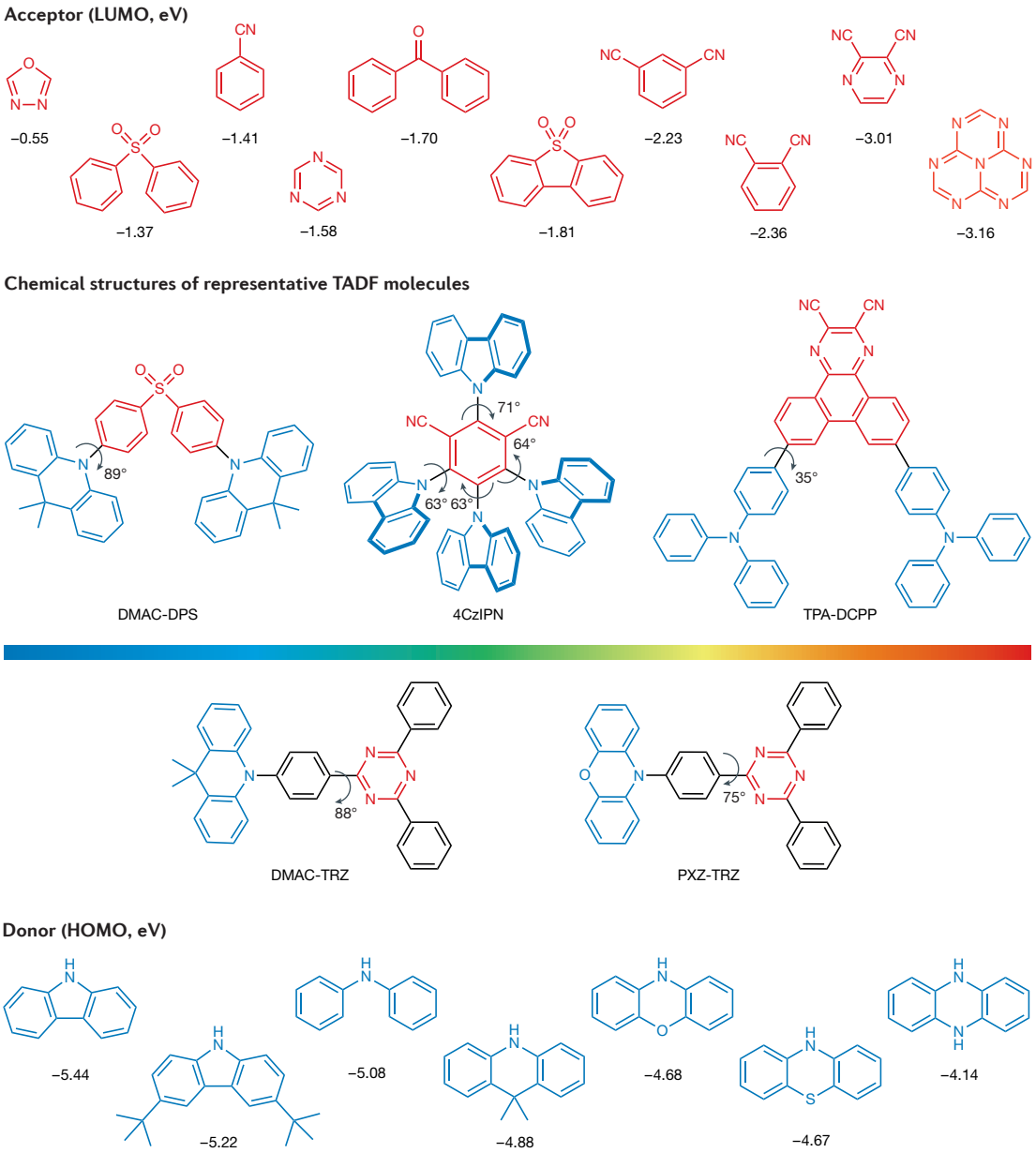

Figure 3 | **Chemical structures of representative acceptors, donors and TADF small molecules.** The colour bar indicates the emission wavelength of the molecules. These molecules include the deep-blue emitter DMAC-DPS (464 nm), the sky-blue emitter DMAC-TRZ (495 nm), the green emitter 4CzIPN (507 nm), the green-yellow emitter PXZ-TRZ (545 nm) and the red emitter TPA-DCPP (708 nm). The dihedral angles between electron donor and acceptor moieties are shown in the molecular structures. HOMO, highest occupied molecular orbital; LUMO, lowest unoccupied molecular orbital; TADF, thermally activated delayed fluorescence.

Photoluminescence. DF arising from triplet states is closely related to the environment because the emission is easily quenched by oxygen[25]. Therefore, the photoluminescence intensity of TADF emitters is higher under vacuum than in oxygen. The calculated emission ratio ($I_{Vac}/I_{O_2} = (I_{PF} + I_{DF})/I_{PF} = I_{DF}/I_{PF} + 1$) can effectively express the contribution from the triplet state. Additionally, TADF emitters show solvatochromic behaviour. For example, a yellow TADF emitter, 2,8-bis[*N*,*N*-di(4-butylphenyl) amino]dibenzothiophene-*S*,*S*-dioxide, shows strong and well-resolved emission in hexane, assigned to an excited state with strong $^1\pi\pi^*$ character[21]. By contrast, in ethanol, the emission is broadened and redshifted, owing to a redistribution of the electron density in the intramolecular ^{1}CT state.

There have been many molecular design strategies to enhance the PLQY of TADF emitters. A smaller ΔE_{ST} can contribute to a fast RISC process, which is advantageous for a high PLQY. In one approach, a phenyl linker is used to increase the CT character from the donor to the acceptor in the S_1 state to generate a smaller ΔE_{ST} (REF.[31]). For example, the sky-blue TADF emitter BCzT[60] has a phenyl group inserted between the donor and acceptor of CzT[61]. The LUMO distribution of BCzT is extended

to the electron-donating unit in contrast to CzT, which resulted in a higher PLQY for BCzT (95.6%) than for CzT (39.7%) measured in DPEPO films. Dispersing the HOMO distribution is another way to improve the PLQY because this increases the oscillator strength. For example, a series of blue TADF emitters containing the TRZ acceptor together with different carbazole donors (Ph3Cz-TRZ, 3Cz-TRZ and 2Cz-TRZ) displayed PLQYs of 100%, 95% and 93% in DPEPO films, respectively, as Ph3Cz-TRZ has the widest HOMO distribution[62].

A narrow emission spectrum with high colour purity is advantageous in display applications. In general, CT excited states can be generated with a range of energies, resulting in very broad emission spectra. Molecular design strategies to achieve a narrow emission spectrum include a rigid, planar core structure or a sterically hindered structure[32,33]. DABNA-1-based OLEDs exhibit emission at 459 nm with a full width at half maximum of 28 nm and CIE coordinates of (0.13, 0.09)[32]. Because of the rigid triphenylboron π-conjugated framework, nitrogen and boron atoms exhibit opposite resonance effects, and a separation of the HOMO and LUMO states occurs at high oscillator strength. A deep-blue TADF device based on CzBPCN shows electroluminescence at 460 nm with a full width at half maximum of 48 nm and an EQE_{max} of 14.0%[33]. At the biphenyl core, two carbazole units of CzBPCN are interlocked because rotation of the biphenyl unit is sterically prohibited.

Characteristics of singlet–triplet energy splitting. TADF small-molecule OLEDs benefit from a small ΔE_{ST} and a short τ_{DF}. In general, ΔE_{ST} is estimated experimentally from the onsets of the fluorescence and phosphorescence spectra for the ^{1}CT and ^{3}CT states and from the peak maxima of the phosphorescence spectra for triplet states when ^{3}LE transition character is dominant. In addition, ΔE_{ST} can be calculated by fitting an Arrhenius plot of k_{RISC} as a function of $1/T$, according to equation 1.

Many methods have been developed to optimize these properties, as described below.

Strong donors or acceptors can attain a small exchange energy and small ΔE_{ST} owing to the increased CT character and stabilization of the singlet energy. A green-emitting Px-VPN with stronger donor units than Cz-VPN achieves a smaller ΔE_{ST} of 0.08 eV and a shorter τ_{DF} of 2.3 µs, compared with 0.36 eV and 173 µs for Cz-VPN, in mCBP films[63]. The HOMO–LUMO energy gap decreases from 3.2 eV (Cz-VPN) to 2.3 eV (Px-VPN) because the electron-donating ability of their donor units affects their HOMO energy levels. Analogously, Px-CNP, which contains a strong electron-withdrawing dicyanopyrazine core, has a lower LUMO energy and larger electron affinity, resulting in a shorter τ_{DF} (1.5 µs) and smaller ΔE_{ST} (0.04 eV) than its phthalonitrile-based counterpart[63].

Emitters with multiple donors or multiple acceptors can also effectively decrease ΔE_{ST} and τ_{DF}. Examples are the blue TADF emitters DTC-pBPSB and DTC-mBPSB, which have two sulfonyl groups as acceptors and 3,6-di-tert-butylcarbazole as the donor. These emitters have comparatively small ΔE_{ST} values (0.19 and 0.26 eV, respectively) and short τ_{DF} values (1.23 and 1.16 µs, respectively) in neat films (that is, undoped films)[64]. Their single sulfonyl counterpart, tDCz-DPS, exhibits a larger ΔE_{ST} (0.32 eV) and a considerably longer τ_{DF} (270 µs) in neat films[8]. Similarly, donor–acceptor–donor-type molecules generally have a smaller ΔE_{ST} and a shorter τ_{DF} than their corresponding donor–acceptor analogues[65].

A distorted backbone structure between the donor and acceptor units is also beneficial to decreasing the ΔE_{ST}. Therefore, an *ortho*-phenyl linkage is better than a *meta*-linkage or *para*-linkage. This is illustrated with a series of benzofurocarbazole (BFCz) donor and TRZ acceptor molecules: the *ortho*-linkage, *meta*-linkage and *para*-linkage isomers have ΔE_{ST} values of 0.002, 0.30 and 0.19 eV, respectively, in DPEPO films[36].

Another method to obtain a small ΔE_{ST} is to use a through-space (that is, non-covalent) interaction[66]. For example, TPA-QNX(CN)2 (TABLE 1), which has a homoconjugated structure, has a ΔE_{ST} of 0.111 eV and τ_{DF} of 2.4 µs in cyclohexane. In addition, the maximum emissions of TPA-QNX(CN)2 are located at 554 nm in toluene and 601 nm in the pure film, which shows that different properties of the isolated molecules and large ensemble of molecules can be attributed to the solid-state solvation effect. Homoconjugation has also been used in spiro-based TADF emitters. For example, spiro-CN shows a small ΔE_{ST} (0.057 eV) and short τ_{DF} (14 µs) in a mCP film, because the donor and acceptor are orthogonally connected via a spirobifluorene moiety[67].

Despite the examples provided above, it is possible to achieve good OLED performance with a relatively large ΔE_{ST} and long τ_{DF}. For example, the blue–green emitter HMAT-TRZ, which contains azatriangulene and diphenyltriazine moieties, has a ΔE_{ST} of 0.38 eV, τ_{DF1} of 0.7 ms and τ_{DF2} of 7.18 ms. The doped mCBP film also has a high PLQY of 84.7%[68].

OLED fabrication and performance

Doped TADF-based OLEDs. In TADF-based OLEDs, the emitter is usually dispersed in a solid host matrix at a relatively low concentration to avoid exciton annihilation. Host materials should be carefully chosen to have the following features: a higher triplet energy than the TADF emitter, suitably aligned HOMO and LUMO, a large bandgap, bipolar charge-transport properties to maximize exciton formation in the emitter layer and minimize exciton quenching at the electrode interfaces, high morphological stability and good film-forming properties[69].

In most cases, traditional host materials — initially developed for heavy metal phosphorescent complexes[70] — are used in the fabrication of OLEDs with TADF emitters. Typical hosts with high triplet energies include DPEPO (T_1: 3.3 eV)[26], PPF (T_1: 3.1 eV)[63], mCPCN (T_1: 3.03 eV)[71], CzSi (T_1: 3.0 eV)[71], PPT (T_1: 3.0 eV)[72], mCP (T_1: 2.9 eV)[26], mCBP (T_1: 2.9 eV)[62], TPBi (T_1: 2.7 eV)[73] and CBP (T_1: 2.64 eV)[26] (Supplementary Figure S2). Several host materials[74–76] have been developed for the high-efficiency green emitter 4CzIPN, for which an EQE_{max} of 31.2% was reported (TABLE 1). Many host materials[77,78] for the blue emitter DMAC-DPS have been designed. Most notably, an EQE_{max} of 23.0% was obtained with

Table 1 | **Photoluminescence and electroluminescence characteristics of representative small-molecule TADF materials**

Molecule	Medium	λ_{PL} (nm)	ΔE_{ST} (eV)	Φ_{PL} Host/ toluene (%)	τ_{PF} (ns)/ τ_{DF} (μs)	CE (cd A^{-1})	PE (lm W^{-1})	EQE_{max} (%)	Refs
DMAC-DPS	PL: mCP film (10 wt%)	464	0.09	90/80	21/3.1	–	–	19.5	26
	EL: DPEPO film (10 wt%)								
	mCP film (10 wt%)					–	19	19.5	87
	PL: mCP film (10 wt%)					39.7	44.4	23.0	79
	EL: DPEPO film (10 wt%)								
DMAC-TRZ	mCPCN film (8 wt%)	495	0.05	90/83	20.3/1.9	66.8	65.6	26.5	30
	PL: mCPCN film (10 wt%)					61.1	45.7	20	30
	EL: neat film								
4CzIPN	CBP film (6 wt%)	507	0.08	93.8/–	17.8/5.1	–	–	19.3	6
	3CzPFP (1%)					–	–	31.2	46
PXZ-TRZ	CBP film (6 wt%)	545	0.08	66/43	20/1.1	–	–	12.5	58
DACT-II	CBP film (9 wt%)	529	0.009	63.7/100	–/–	–	–	29.6	59
TPA-DCPP	Neat film	708	0.13	14/84	20.8/0.76	4.0	–	9.8	19
HAP-3TPA	26mCPy film (6 ± 1 wt%)	610	0.17	91/–	–/100	25.9	22.1	17.5	28
BCzT	DPEPO film (6 wt%)	483	0.31	95.6/–	5.5/33	–	–	21.7	60
Ph3Cz-TRZ	DPEPO film (6 wt%)	480	0.09	100	6.3/–	–	–	20.6	62
Px-VPN	mCBP film (6 wt%)	540	0.08	77/42	27/2.3	45.4	26.7	14.9	63
TPA-QNX(CN)2	PL: toluene or cyclohexane for τ_{DF}	554	0.111	44/–	–/2.4	–	–	9.4	66
	EL: mCP film (10 wt%)	601							
DABNA-1	PL: neat film	460	0.20	88/–	8.8/93.7	10.6	8.3	13.5	32
SpiroAC-TRZ	mCPCN film (12 wt%)	480	0.072	100/–	17/2.1	94	98.4	36.7	29
DMAC-BP	mCP film (10 wt%)	498	0.07	90/85	–/3.0	–	59	18.9	87
DBT-BZ-DMAC	PL: neat film	505	0.08	80/–	40.4/2.9	51.7	50.7	17.9	88
	EL: CBP film (6 wt%)								
	Neat film					43.3	35.7	14.2	88
ACRDSO2	PL: neat film or CBP film (6 wt%) for τ_{PF}/τ_{DF}	578	0.058	71/34	36/8.3	61.8	54.0	19.2	98
	EL: CBP film (6 wt%) and evaporation process								
	PL: neat film or CBP film (6 wt%) for τ_{PF}/τ_{DF}					53.3	–	17.5	98
	EL: CBP film (6 wt%) and solution process								
PXZDSO2	PL: neat film or CBP film (6 wt%) for τ_{PF}/τ_{DF}	608	0.048	62/37	36/5.0	49.3	38.5	16.7	98
	EL: CBP film (6 wt%) and evaporation process								
	PL: neat film or CBP film (6 wt%) for τ_{PF}/τ_{DF}					45.1	–	15.2	98
	EL: CBP film (6 wt%) and solution process								

CE, maximum current efficiency; EL, electroluminescence; EQE_{max}, maximum external quantum efficiency; ΔE_{ST}, singlet–triplet energy splitting; PE, maximum power efficiency; PL, photoluminescence; TADF, thermally activated delayed fluorescence; Φ_{PL}, photoluminescence quantum yield; λ_{PL}, wavelength of maximum photoluminescence; τ_{DF}, delayed fluorescence lifetime; τ_{PF}, prompt fluorescence decay lifetime. '–' indicates that the reference did not provide the data.

DPETPO as the host[79]. Polar hosts can stabilize the CT excited state of the guest emitter owing to local dipole interactions and thereby redshift the emission. For example, host–guest interactions have been studied in detail for the blue TADF emitter DDMA-TXO2. By combining the emitter with a host of the correct polarity, the energy of the ^{1}CT state is lowered, and the ΔE_{ST} is minimized, resulting in an EQE_{max} of 22.4% for a device with CIE coordinates of (0.16, 0.24)[80].

White TADF OLEDs are a growing area of research[81–83]. For example, mixing green (4CzPN), red (4CzTPN-Ph) and blue (3CzTRZ) emitters with hosts (mCBP and PPT) in the emitting layer gives white OLEDs[81]. With an optimized light-emitting layer composed of 4CzPN:mCBP (3 nm)/4CzTPN-Ph:mCBP (2 nm)/3CzTRZ:PPT (10 nm), the device achieved an EQE_{max} of 17.6% and $CIE_{x,y}$ of (0.26, 0.38). In addition, phosphorescent and fluorescent emitters have also been doped to prepare TADF white OLEDs. Hybrid 'warm-white' OLEDs using the blue TADF emitter 2CzPN and yellow phosphor PO-01 in separate emitting layers (FIG. 4a; Supplementary Figure S1) achieved an EQE_{max} of 22.6% ($CIE_{x,y}$ = (0.45, 0.48))[82]. By combining the yellow TADF emitter PXZDSO2 with the deep-blue fluorescence emitter NI-1-PhTPA,

two-colour warm-white OLEDs were prepared, achieving an EQE_{max} of 15.8% ($CIE_{x,y}$ = (0.401, 0.477)) with a colour rendering index (CRI) of 68 (REF.[83]). Furthermore, when a deep-red fluorescent component was introduced, three-colour white OLEDs were obtained with an EQE_{max} of 19.2% ($CIE_{x,y}$ = (0.348, 0.577)), a very high CRI of 95 and an EQE of 15.6%[83].

Oriented molecules can enhance the efficiency of doped devices[84]. An emitter with a horizontal transition dipole moment results in a much higher out-coupling efficiency than the vertically aligned dipole, and hence higher EQE[85]. Theoretically, it is possible to increase the EQE up to 46% for perfectly horizontally oriented emitters without the use of external out-coupling structures with $\Phi_{PL} = 1$ and $\Theta = 1$, where Φ_{PL} is the PLQY and Θ is the percentage of horizontal dipoles among all emitting dipoles (REF.[84]). For example, combining the host DPEPO and TADF emitter CC2TA as the emitting layer resulted in an EQE_{max} of 11 ± 1% owing to the high percentage of all emitting dipoles (Θ = 92%)[86] (FIG. 4b). The out-coupling efficiency of the emitters arranged horizontally (31.3%) was higher than that of the isotropic emitters (20.6%). In another example, the TADF emitter spiroAC-TRZ, which has strongly horizontally oriented emitting dipoles (Θ = 83%), displayed extremely efficient electroluminescence with an IQE of nearly 100% and an EQE of 37%[29].

Non-doped TADF-based OLEDs. Non-doped emitter layers are more attractive than doped (host–guest) systems for two reasons. First, the fabrication processes are easier. Second, heterogeneities (such as those that arise from phase separation of the components), which are detrimental to colour stability and device efficiency, cannot occur. However, non-doped OLEDs are relatively rare. Most non-doped devices exhibit a lower voltage, higher luminance and smaller efficiency roll-off than the corresponding doped devices. Holes and electrons recombine efficiently into excitons within the broader recombination zone of a neat film owing to the superior bipolar charge-transport properties of TADF molecules[30]. In addition, increasing the doping concentration can lower the probability of an emitter being in its excited state and thus reduce excitation-dependent dissociation[87]. The shorter decay lifetime of DF in a neat film can also help to decrease efficiency roll-off[88].

Non-doped green and blue OLEDs employing DMAC-BP and DMAC-DPS displayed EQEs and a highest luminance of 18.9% and ~50,000 cd m^{-2}, and 19.5% and 100 cd m^{-2}, respectively[87]. The blue emitter DMAC-TRZ attained an EQE of 18.9% at a brightness of 100 cd m^{-2} in non-doped OLEDs[30]. OLEDs based on DBT-BZ-DMAC, showing combined aggregation-induced emission and TADF, displayed an EQE_{max} of 14.2% and a negligible current efficiency roll-off of 0.46% from the peak values to those at 1,000 cd m^{-2} (REF.[88]). In a recent example, the green luminogen CP-BP-PXZ, which exhibits aggregation-induced DF properties, was used in a non-doped OLED. This device displayed an EQE of 18.4%, with a negligible current efficiency roll-off of 1.2% at 1,000 cd m^{-2}; these data are comparable to those of doped devices[89].

TADF exciplex OLEDs are another kind of non-doped device (FIG. 4c; Supplementary Figure S3). An exciplex is a CT state, and its emission occurs as a result of an electron transition from the LUMO of the accepter to the HOMO of the donor under photoexcitation and electrical excitation[7]. The intermolecular excited states (that is, exciplex state) should provide a smaller exchange energy than the intramolecular excited states, resulting in the triplet levels being very close to the singlet levels[7]. The first reported TADF exciplex emission was from *m*-MTDATA:3TPYMB, which demonstrated an EQE of 5.4%. Furthermore, the triplet exciplex state must be confined using donor and acceptor molecules with high triplet energy levels to decrease triplet state quenching. OLEDs based on exciplex emission from *m*-MTDATA-:PPT achieved an EQE_{max} of 10.0%[90]. These results suggest that high-PLQY exciplex emitters are required for further efficiency improvement. The TAPC:DPTPCz exciplex system with high T_1 triazine/carbazole exhibited a high PLQY of 68%, a small ΔE_{ST} of 0.047 eV and an EQE of 15.4% in a green OLED[91]. The best-performing device based on an exciplex is that of MAC:PO-T2T, which achieved an EQE_{max} of 17.8%. In this design, two RISC channels on both the pristine TADF MAC molecules and the exciplex system can be utilized[92].

Solution-processed TADF-based OLEDs. OLEDs with a solution-processed emitter layer have attracted attention for large-area displays owing to their simple fabrication processes and relatively low cost. The performance of solution-processed OLEDs is generally inferior to that of vacuum-deposited OLEDs[93] (FIG. 4d). Recently, a few TADF OLEDs with good performance have been fabricated by the solution processing of small molecules. The solubility of small molecules in aromatic solvents can be improved to apply solution fabrication techniques by introducing methyl groups[71], tert-butyl groups[71], fluorine atoms[94], trifluoromethyl groups[95] or sec-butoxy groups[96]. Other TADF molecules that are applicable for solution processing without specific solubilizing groups include 3ACR-TRZ, ACRDSO2 and PXZDSO2 with an EQE_{max} of 18.6%[97], 17.5%[98] and 15.2%[98], respectively (FIG. 4d). The HOMO levels are estimated to be −5.26 eV for ACRDSO2 and −5.06 eV for PXZDSO2. Compared with PXZDSO2, the weaker electron-donating group lowers the HOMO level of ACRDSO2, which matches well with the HOMO level of the CBP host, leading to improved device performance.

Device stability. In addition to high-performance light-emitting characteristics, a long operational lifetime under electrical excitation is necessary for commercial applications. Suppressing the degradation of hole-transport and electron-transport materials has a positive effect on the lifetime of a device, because this ensures that charges are effectively confined in the emitting layer owing to large energy barriers for hole and electron leakage[53]. In addition, reduction of charge accumulation at the interface between the emitting layers and the charge-transport layers can reduce exciton–polaron quenching, thereby enhancing the device

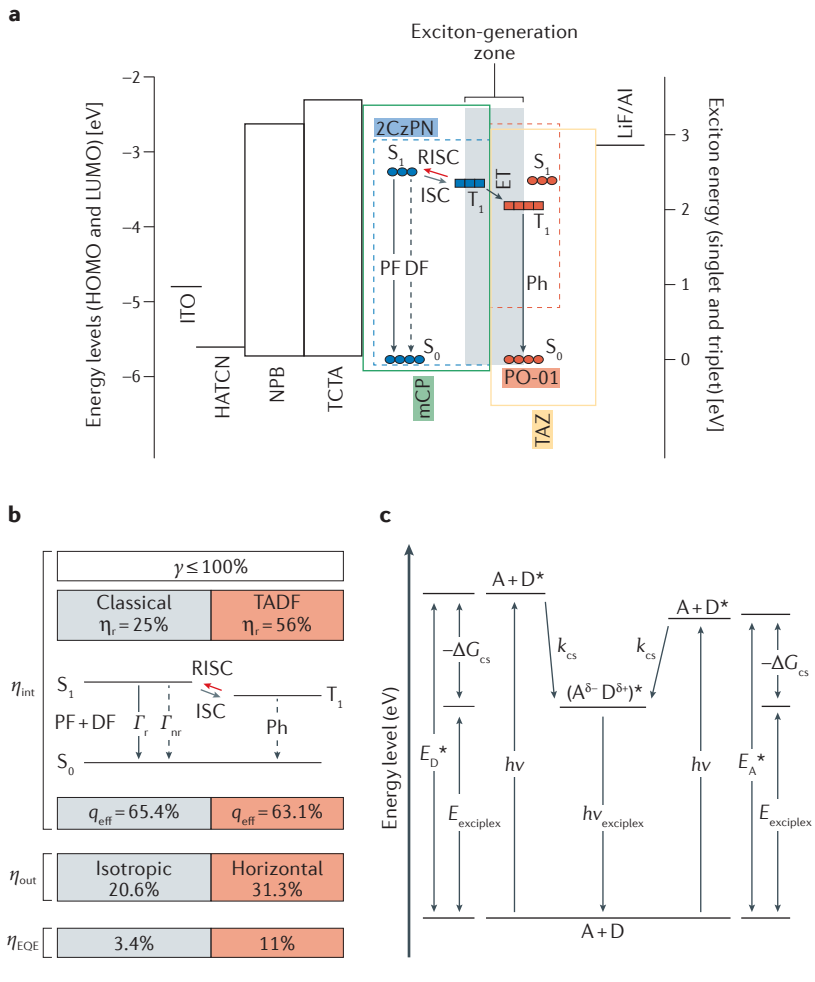

d

TADF molecule	Solution process	Evaporation process
	ITO/PEDOT:PSS | EML | TmPyBP | LiF/Al	ITO/HATCN | TAPC | EML | TmPyBP | LiF/Al
ACRDSO2	17.5%	19.2%
PXZDSO2	15.2%	16.7%

Figure 4 | **The performance of small-molecule TADF OLEDs. a** | Energy levels, exciton energies and the mechanism of light emission for materials used in hybrid white organic light-emitting diodes (OLEDs). A hybrid white OLED has two emitting layers (EMLs). The first EML, which is close to the hole-transporting layer (NPB), contains 2CzPN in a mCP host. In the second EML, which is close to the electron-transporting layer, PO-01 is doped in the host. The emitting layers are sandwiched between the electron-transporting layer of TAZ and the electron/exciton-blocking layer of TCTA. HATCN is used as the hole-injection layer. The large energy offset of the highest occupied molecular orbital (HOMO) of TAZ and the HOMO of mCP prevents hole transport between the adjacent hole-transporting layer. In the exciton-generation zone (grey), a hole and an electron can combine via Coulomb forces to form excitons. **b** | Individual contributions of isotropic and horizontal singlets to the external quantum efficiency (EQE or η_{EQE}) in the oriented EML. The left column lists typical values for an isotropic singlet emitter, and the right column lists typical values for an oriented thermally activated delayed fluorescence (TADF) emitter enabling EQE beyond the classical limit. TADF increases the percentage of radiative exciton, η_r, as a consequence of the up-conversion of triplet excitons to the singlet state, which in turn boosts the internal quantum efficiency (η_{int}). The horizontal orientation of the transition dipole moments in the EML increases the out-coupling efficiency (η_{out}). It is assumed that the radiative quantum efficiency is the same in both scenarios. However, because Purcell factors depend on orientation, slightly different radiative quantum efficiency values are used in the calculation of η_{EQE}. **c** | Electronic energy diagram showing the exciplex formation process and energy-level relationships. First, donors and acceptors form excited donors and ground state acceptors or form excited acceptors and ground state donors under high-energy excitation. Then, donor excitons and acceptor excitons combine into an exciplex. Finally, the exciplex decays into light and ground state donors and acceptors. **d** | Device structures and EQEs of vacuum-deposited and solution-processed OLEDs based on ACRDSO2 and PXZDSO2. The structures of HATCN, NPB, TCTA, 2CzPN, mCP, PO-01, TAPC and TAZ are given in Supplementary Figures S1–S4. A, acceptor; D, donor; DF, delayed fluorescence; E_{A*}, exciton energy of the acceptor; E_{D*} exciton energy of the donor; $E_{exciplex}$, exciplex photon energy; ET, triplet energy; $-\Delta G_{cs}$, driving force; ISC, intersystem crossing; k_{cs}, rate constant of exciplex formation; LUMO, lowest unoccupied molecular orbital; PF, prompt fluorescence; Ph, phosphorescence decay; q_{eff}, effective radiative quantum efficiency; RISC, reverse intersystem crossing; γ, charge balance factor; Γ_r, radiative decay rates of the emitting molecule; Γ_{nr}, non-radiative decay rates of the emitting molecule; $h\upsilon$, optical radiation. Panel **a** is adapted with permission from REF.[82], RSC. Panels **b** and **d** are reproduced with permission from REFS[86,98], Wiley-VCH. Panel **c** is adpated with permission from REF.[91], Wiley-VCH.

stability[54]. The chemical stability of the molecules[99] and the matching of energy levels between hosts and emitters[53] can also contribute to long device lifetimes. For example, a DCzDCN:4CzIPN (15 wt%) device had a lifetime of 200 hours with up to 90% of the initial luminance of 1,000 cd m^{-2} (LT_{90}/1,000). By contrast, a CBP:4CzIPN (15 wt%) device exhibited a lifetime of only 10.2 hours under the same conditions. This is because the low singlet energy of 2.88 eV for DCzDCN increases the energy-transfer efficiency during the light-emission process[54]. Devices composed of SF34:4CzIPN (8 wt%) exhibited considerably longer lifetimes (LT_{80}/2,000) of 252.4 hours, compared with the control device using CBP as the host (61.5 hours). This indicates that pure

hydrocarbon hosts have good electroluminescence stability and a suitable glass transition temperature for OLEDs[100]. Electron-transporting n-type hosts can efficiently increase the lifetime of OLEDs, as mentioned earlier. Following this strategy, a sky-blue TADF OLED with a high EQE of 8.8% and a lifetime of 454 hours was produced[35]. This lifetime is three orders of magnitude higher than that of the device hosted by the p-type material CzSi (REF.[101]).

Dendritic TADF materials

Structure and photophysical features

Dendrimers have been widely used in organic optoelectronics because of their solution processability, homogeneous film morphology, relatively high molecular weight but precise molecular structure, and tuneable energy gap and emission colour (by controlling the numbers of dendrons)[102,103]. In this section, we outline guidelines for controlling the photophysical properties and device performance of TADF dendrimers, followed by specific examples. The structures of the materials covered are shown in Supplementary Figure S5, and TABLE 2 provides their photoluminescence and electroluminescence performances.

Star-shaped or dendrimer TADF emitters are typically composed of a TADF core with branched, dendritic molecular structures (namely, dendrons) attached. These dendrons isolate the core and prevent concentration quenching and efficiency roll-off caused by intermolecular interactions and exciplex formation. TADF dendrimers are classified into either conjugated[104–108] or non-conjugated structures[109–114], depending on the functional group that links the core to the dendrons. A drawback of π-conjugated linkages between the core and dendrons is that this can lead to reduced solubility and a change in the emission colour compared with that of the isolated core. Therefore, non-conjugated structures are preferable. An example of this class of structure is a TADF core and carbazole dendrons connected through non-conjugated aliphatic chains[109] (**D7**; TABLE 2), which has good solubility and charge-transport ability but maintains the emission of the TADF core[115,116].

In general, ΔE_{ST} depends on the TADF core and is not significantly affected by the generation (that is, the number of repeated branching cycles) of the dendrimers, especially for non-conjugated structures[109,110]. Carbazole dendrons are typically used to minimize concentration quenching or triplet–triplet annihilation because of the good hole-transport properties[117], high triplet energy[103], thermal stability[118,119] and excellent crosslinking ability[120,121] of carbazole. Yamamoto and co-workers[104] reported the first conjugated nonpolar TADF dendrimer, which was a second-generation dendrimer containing a triphenyl-*s*-triazine acceptor core and multiple donor carbazoles (**D1**; FIG. 5; TABLE 2). In addition, DMAC-DPS emitters encapsulated by multiple carbazoles (**D2**; TABLE 2) exhibit blue emission with TADF characteristics, high PLQY and excellent photophysical and electroluminescent properties[105]. In some cases, TADF dendrimers with carbazole dendrons show a significantly reduced ΔE_{ST}, favouring efficient RISC[104,105], which is ascribed to an extended potential gradient. In addition, substituents or end groups also affect ΔE_{ST}. For example, methyl, tert-butyl and phenyl favour efficient CT processes from donor to acceptor in the S_1 state and give a small ΔE_{ST} for TADF dendrimers. Moreover, a series of terminally substituted dendrimers exhibit a slightly smaller ΔE_{ST} than their unsubstituted analogues[106] (**D5**, **D6**; TABLE 2). In addition to peripheral carbazole dendrons, bipolar groups balance carrier transport and thus improve the efficiency. For example, a blue TADF dendrimer[110] (**D9**; FIG. 5; TABLE 2) in which DMOC-DPS serves as the TADF core and POCz as the bipolar dendrons exhibited excellent charge-transport properties. In another example, alkyl chains were introduced as bridges between the core and dendrons to retain the frontier orbital distribution of the components and the colour purity of the TADF core[110].

TADF dendrimers exhibit more complex photoluminescence spectral characteristics than individual TADF components. This is particularly the case for conjugated dendrimers: with increasing dendrimer generation, the HOMO migrates from the internal donor moieties to the peripheral dendrons, while the LUMO remains located on the acceptors. Consequently, the distance between the HOMO and LUMO levels increases and the absorption coefficient of the CT band decreases. However, the photoluminescence spectra are almost identical for dendrimers with different generations. As previously demonstrated[104], emission from a CT state is related only to the neighbouring carbazole moieties of the TADF core because of a highly twisted spatial structure. Nevertheless, in some cases, the HOMO will delocalize over both the donor moieties and the peripheral dendrons owing to a relatively planar conjugated structure. For example, the photoluminescence emission of DCzDMAC-DPS[105] (**D3**, TABLE 2) shows a slight blueshift compared with the DMAC-DPS core, whereas a slight redshift for CzDMAC-DPS (**D2**, TABLE 2) is observed. This can be explained in terms of the different distributions of the HOMO, in contrast to the LUMO, which remains located on DPS. For non-conjugated TADF dendrimers, the absorption bands induced by intramolecular CT and the emission peaks from the lowest excited singlet state are essentially unchanged (that is, the TADF core behaves independently of the peripheral dendrons)[109,110]. Dendrimers also exhibit distinct solvatochromic effects with a weaker solvent-dependent shift than their small-molecule counterparts, which can be attributed to the reduced interactions between solvent molecules and the encapsulated emissive core[110]. The temperature dependence of transient photoluminescence decay in dendrimers is generally the same as that of their small-molecule counterparts (that is, DF gradually increases with temperature)[104]. Nevertheless, the contribution of the DF slightly decreases at high temperature, which might be caused by increased non-radiative processes[104].

The dendrimer generation has a marked effect on the DF and PLQY. The DF proportion of nonconjugated TADF dendrimers is higher than that of the corresponding TADF monomers. This is because reduced quenching by molecular encapsulation facilitates the RISC

Table 2 | **Summary of the photoluminescence and electroluminescence characteristics of representative dendrimer TADF materials.**

Dendrimer	λ_{max} (nm)	ΔE_{ST} (eV)	Φ_{PL}/Φ_{DF} (%)	τ_{PF} (ns)/ τ_{DF} (μs)	V_{on} (V)	L_{max} (cd m^{-2})	CE (cd A^{-1})	PE (lm W^{-1})	EQE$_{max}$ (%)	CIE (x, y)	Refs
D1	475[a], 500[d]	0.06	59[a], 100[b], 31[c]/24.8	–/–	3.5	~1,000	8.5	–	3.4	(0.27, 0.49)	104
D2	498[a], 492[d]	0.09	67.5[c]/–	28.5/1.54	3.6	~3,000	30.6	24.0	12.2	(0.22, 0.44)	105
D3	464[d]	0.20	0.48[c]/–	25.8/1.91	5.2	~500	3.8	2.0	2.2	(0.18, 0.27)	105
D4	520[d]	0.11	77[c]/–	15/0.523	4.4	>10,000	38.9	17.3	13.8	(0.40, 0.54)	49
D5	422	0.07	62[a], 92[b] 40[c]/2/11[c]	15.7/3.3	3.0	2,235	26.5	21.5	9.4	–	106
D6	422	0.07	63[a], 96[b], 45[c]/14	13.3/5.3	3.5	2,423	25.4	16.1	9.5	–	106
D7	535[a], 487[d]	0.20	76[c]/–	16/–	3.6	22,950	30.5	–	10.1	(0.24, 0.51)	109
D8	591[a], 541[d]	0.20	71[c]/–	16/0.8	2.4	23,145	39.0	40.8	11.8	(0.39, 0.56)	111
D9	490[a], 460[d]	0.23	61/–	–/–	5.4	2,700	12.6	–	7.3	(0.18, 0.30)	110
D10	395[a], 517[a], 520[d]	0.079	69.2[c]/33.8	21.7/2.9	4.0	2,336	30.8	24.2	9.5	(0.32, 0.57)	112
D11	392[a], 412[a], 495[a], 494[d]	0.134	59.4[c]/27.3	16.1/25.2	4.5	2,770	20.7	14.5	8.1	(0.22, 0.43)	112
D12	527[a], 548[d]	0.08	90/–	16/1.0	2.7	18,800	44.5	46.6	16.5	(0.42, 0.55)	113
D13	452[a], 475[d]	0.22	78[b], 25[a]/–	2.8/4.5	3.5	7,800	48.6	35.2	23.5	(0.15, 0.30)	52

[a]Measured in solution in air. [b]Measured in solution under N_2. [c]Measured in film under N_2. [d]Measured in film in air. CE, maximum current efficiency; CIE, Commission Internationale de l'Éclairage; EQE$_{max}$, maximum external quantum efficiency; ΔE_{ST}, singlet–triplet energy splitting; L_{max}, maximum luminance; PE, maximum power efficiency; TADF, thermally activated delayed fluorescence; V_{on}, turn-on voltage at 1 cd m^{-2}; Φ_{DF}, delayed fluorescence quantum yield; Φ_{PL}, photoluminescence quantum yield; λ_{max}, wavelength of maximum luminescence; τ_{DF}, delayed fluorescence lifetime; τ_{PF}, prompt fluorescence decay lifetime. '–' indicates that the reference did not provide the data.

and radiative deactivation processes of triplet excitons. The proportion of DF in solution generally increases with increasing generation of dendrimer; for example, the contributions of DF at 300 K were calculated to be 43% for a second-generation dendrimer (**D1**; TABLE 2) and 81% for a third-generation dendrimer[104]. However, for higher generations, the proportion of DF decreases, possibly owing to the long lifetime and quenching of excitons. Moreover, TADF dendrimers with higher generations usually result in lower PLQY. This can be ascribed to the long photoluminescence lifetime and increased exciton quenching caused by intermolecular interactions[112] (**D10**, **D11**; TABLE 2).

OLED fabrication and performance

The EQEs of solution-processed dendrimer devices are still rather low, and further work is required to realize high-efficiency devices[104,122]. However, in some cases, dendrimer emitters can exhibit higher luminescence and a lower turn-on voltage than their small-molecule counterparts[49,109]. The TADF core is the main factor that determines the device efficiency. For example, a DMAC-DPS core encapsulated by multiple carbazoles exhibited an EQE$_{max}$ of 12.2% and brightness of ~3,000 cd m^{-2} (REF.[105]). By replacing the core with DMAC-BP (**D4**; TABLE 2), the non-doped OLEDs exhibit a slightly higher EQE of 13.8% and brightness over 10,000 cd m^{-2} (REF.[49]), which can be partly ascribed to the full harvesting of excitons generated from TADF and exciplex formation[123]. In addition to the TADF core, dendrimer generation is an important factor. A higher dendrimer generation usually improves the charge injection and transport and suppresses exciton quenching owing to the more effective encapsulation of the emissive core. As a result, exciton recombination is more efficient, resulting in reduced efficiency roll-off. TADF dendrimers with selective interfacial exciplex-forming dendrons can lead to relatively efficient solution-processed OLEDs[113] (**D12**; TABLE 2). An exciplex, which can be formed at the interface between hole-transporting dendrons and the adjacent electron-transport layer, will effectively boost charge injection and transport to the TADF core.

The structures of the linkage between the core and dendrons can affect the device efficiency. In general, non-conjugated flexible connections not only ensure the relatively independent optical and electrical properties of the subunits but also suppress aggregation and crystallization, thereby favouring amorphous films and improving the

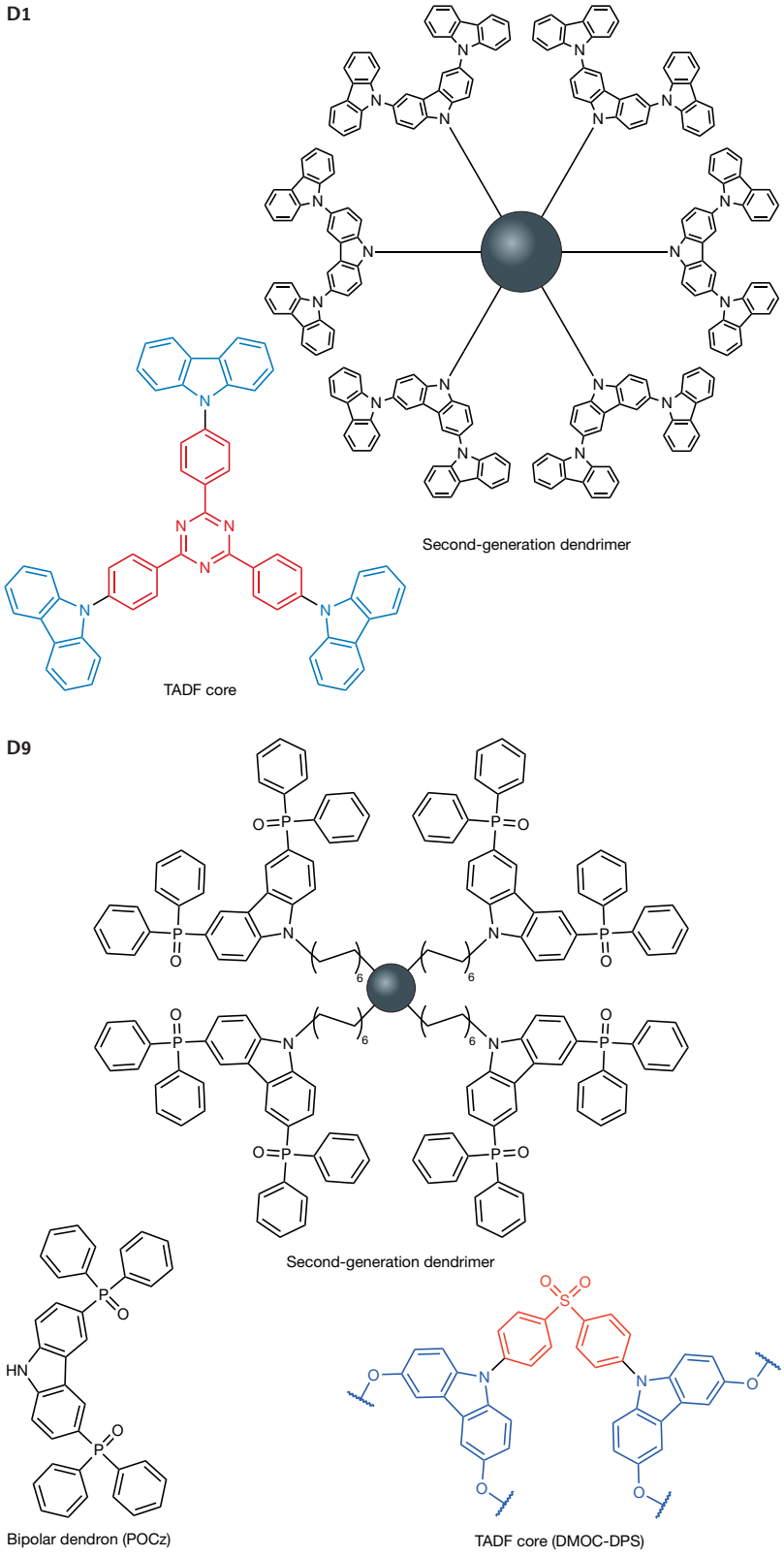

Figure 5 | **Molecular structures of TADF dendrimers.** The conjugated non-polar thermally activated delayed fluorescence (TADF) dendrimer **D1** contains a triphenyl-s-triazine moiety as an acceptor and multiple carbazole groups as donors. **D9** is a dendrimer with bipolar dendrons, in which DMOC-DPS serves as the TADF core and POCz imparts excellent charge-transport properties. Lower panel is adapted with permission from REF.[110], American Chemical Society.

device efficiency. Using this approach, with a TADF core and carbazole dendrons connected by flexible aliphatic chains, an EQE_{max} of 10.1% and a maximum luminance of 22,950 cd m^{-2} was achieved in non-doped OLEDs[109]. This approach can also result in fewer peripheral dendrons contributing to concentration quenching of the TADF core. However, careful selection of peripheral dendrons is important for self-host dendrimers. Tricarbazole dendrons attached to a triazine core lead to better performance than the monocarbazole analogue (**D8**; TABLE 2). OLEDs based on the tricarbazole dendron display a low turn-on voltage of 2.4 V and an EQE_{max} of 11.8%[111]. The low turn-on voltage can be ascribed to the appropriate energy-level matching of the HOMO and the LUMO. In addition, good smooth film forming ability[105] and the favourable molecular orientation of dendrimers significantly enhance device efficiency[106].

For doped dendrimer-based OLEDs, the choice of host is crucial for achieving relatively high device efficiency. For example, instead of using a common, previously used host, a TADF material with an emissive core encapsulated by multiple carbazole dendrons (**D12**; Supplementary Figure S5) was used as the host for **D13** (Supplementary Figure S5). This strategy led to suppression of the energy loss induced by aggregation of the host molecules and the creation of an efficient energy and CT channel with suppressed exciton quenching. The resulting solution-processed blue TADF OLEDs incorporating **D12**:**D13** as the emitting layer exhibited an EQE_{max} of 23.5%[114].

The examples outlined above demonstrate that precise molecular design of the core, linkers and dendron structure, as well as the dendrimer generation, is indispensable for attaining high-efficiency, solution-processed TADF OLEDs.

Polymeric TADF materials

Structure and photophysical features

Thin films of small TADF molecules are usually fabricated by thermal evaporation, which compromises film quality because of the tendency of the molecules to crystallize and aggregate, in turn reducing the efficiency and long-term stability of the OLEDs. By contrast, polymeric and dendritic TADF materials are suitable for film formation by low-cost solution processes, such as spin-coating, die-casting or ink-jet printing[124,125]. However, it is still challenging to prepare polymeric and dendritic TADF materials, and this is an expanding research area. The reason for this difficulty is twofold. First, it is difficult to simultaneously achieve a small ΔE_{ST} and to suppress the nonradiative internal conversion in macromolecules containing a large number of atoms. Second, the triplet excitons generated from TADF are more readily quenched by intermolecular and intramolecular triplet–triplet annihilation in polymers than in small molecules. In addition, a common feature of TADF polymers reported to date is their low molecular weights and high polydispersities, meaning that they are not well-defined materials. To address these issues, many strategies have been applied to the design of TADF polymers[126]. The structures of the materials covered in this section are shown in Supplementary Figure S6,

and TABLE 3 provides their respective photoluminescence and electroluminescence performances.

A simple method for producing TADF polymers is to functionalize and then polymerize a monomer unit that already exhibits TADF characteristics and excellent (small-molecule) device performance. Using this strategy, a series of main chain (that is, TADF units located in the backbone)[127–132], side chain (that is, TADF units as pendant groups)[50,130,133,134], crosslinking[135] and through-space CT (that is, between isolated pendant electron donor and acceptor units rather than intermolecular CT)[136] TADF polymers have been synthesized.

There are several examples of main chain TADF polymers with alternating donor and acceptor units in the backbone or with acceptor units grafted onto a donor backbone. However, TADF is not observed for conjugated polymers in which the donors and acceptors are directly connected to each other in the backbone because of the large ΔE_{ST} of around 0.7 eV (REF.[137]). Therefore, conjugated or nonconjugated spacers are usually inserted to isolate the TADF units and thus reduce ΔE_{ST} and prevent concentration quenching. Stronger electron donor or acceptor units can also reduce ΔE_{ST}. For example, pAcBP (**P3**; TABLE 3), which is based on acridan, has a smaller ΔE_{ST} than pCzBP (**P2**; TABLE 3), which is based on carbazole, because of the stronger electron-donating ability of acridan[127]. Modulating the location of donors and acceptors can also decrease ΔE_{ST}. For example, acceptors were grafted onto a conjugated backbone consisting of alternating electron donors and host moieties[128]. As a consequence, a ΔE_{ST} of 0.37 eV was achieved for PAPCC (**P5**; TABLE 3), and a value of 0.13 eV was achieved for PAPTC (**P6**; TABLE 3).

In the first report of a main chain TADF material (albeit without molecular weight data) (**P1**; FIG. 6; TABLE 3), nonconjugated monomers with high triplet energy were introduced to separate TADF units and prevent quenching of triplet excitons[129]. However, conjugated TADF polymers are much more desirable than main chain TADF polymers with nonconjugated backbones, which suffer from poor charge-transport properties. For example, benzophenone-based conjugated polymers were obtained[127] (**P2**, **P3**; TABLE 3) by adding a third conjugated monomer unit (carbazole and acridan, respectively) as spacers into the donor–acceptor backbones. By grafting acceptor units onto the donor backbone, the twisted donor–acceptor structure also ensures effective TADF. Using this strategy, two conjugated polymers were synthesized containing carbazole and 9,10-dihydroacridine donors in the backbone and cyanobenzene or triazine acceptors as pendants[128] (**P5**, **P6**; TABLE 3). As expected, they exhibited excellent TADF characteristics.

For side chain polymers (TABLE 3; Supplementary Figure S6), the TADF features of monomers can be easily inherited owing to the independent (non-interacting) TADF units. The first nonconjugated side chain polymer with an aliphatic main chain and phenothiazine-dibenzothiophene-*S*,*S*-dioxide TADF pendants (**P8**; TABLE 3) was synthesized by free-radical copolymerization[50,130]. Thus, the near-perpendicular orientation of donors and acceptors within the corresponding small-molecule precursor is retained in **P8** (REFS[50,130]). Typically, efficient TADF units are grafted onto a conjugated carbazole backbone[133,134] (**P9**, **P1**; TABLE 3), and the photophysical features of the polymers are dramatically regulated by controlling the feed ratios of monomers.

Alternative strategies to obtain polymeric TADF materials use thermally crosslinkable TADF materials[135] or conjugation-induced TADF polymers[138] (TABLE 3; Supplementary Figure S6). Specifically, a crosslinked TADF polymer was synthesized by combining crosslinkable vinyl benzyl ether groups with TADF units[135] (**P11**; TABLE 3). In addition, conjugated TADF cyclic oligomers and polymers were synthesized from non-TADF monomers (benzophenone acceptor and carbazole donor[138]) (**P7**; TABLE 3). The TADF characteristics in these polymers are attributed to an extension of the π-conjugated donor, which reduces ΔE_{ST}. Before choosing this method for a TADF polymer, a calculation of the energy levels is desirable for guiding the synthesis. In contrast to traditional TADF polymers, which feature through-bond intramolecular CT, through-space CT can be exploited to separate the HOMO and LUMO and give a relatively narrow ΔE_{ST} (REF.[136]). The first such polymer was based on a nonconjugated polyethylene backbone with through-space CT between the pendant electron donor 9,9-dimethyl-10-phenyl-acridan and acceptor TRZ units[136]. The resulting polymer with 5 mol% acceptor unit displays blue electroluminescence with CIE coordinates of (0.176, 0.269) and an EQE of 12.1%.

TADF polymers show similar photophysical signatures to their small-molecule counterparts, such as solvatochromism, oxygen quenching and CT emission. For example, the I_{Vac}:I_{O_2} ratio of **P8** is 1.35, indicating a strong TADF effect[50]. The polymer **P7** shows fluorescence spanning from blue to yellow in solvents such as toluene, tetrahydrofuran, *o*-dichlorobenzene, chloroform and dichloromethane[138]. Usually, the photoluminescence emission of the donors and acceptors is masked owing to CT processes in the polymers. Thus, polymers typically exhibit much broader spectra than small molecules. In addition, there is often a small redshift of the photoluminescence for polymers because of the increased conjugation. This is exemplified in the absorption and emission spectra of TADF copolymers[130] (**P4**, **P8**; TABLE 3). The photoluminescence intensity increases gradually and redshifts with an increasing ratio of TADF units in the side chain conjugated copolymers **P9** and **P10** (REFS[133,134]). There are also differences between the properties of isolated molecules and large assemblies of molecules, especially for side chain polymers. The molecules in dilute solution are isolated; thus, the emission of the backbone (spacer units) can be observed through energy transfer, which mainly occurs from the backbone to side chain TADF moieties. By contrast, for aggregated molecules in a film, the emission of the backbone is absent, and this can be ascribed to increased intermolecular and intramolecular interactions within the film[133,134].

A common belief about TADF is that triplet excitons are up-converted into singlet states and that delayed singlet excitons then transform radiatively to the ground state. However, in some cases, the calculated thermal

activation energy is much smaller than ΔE_{ST} (REF. 129). T_1 states are locally excited (^{3}LE) states (or regarded as the presence of $^3n\pi^*$), based on the phosphorescence spectra[21]. Accordingly, TADF processes in polymers occur in two stages: an internal conversion from the backbone-centred ^{3}LE into the ^{3}CT state and a RISC from the ^{3}CT to ^{1}CT state.

Unlike small-molecule and dendritic TADF emitters, the PF and DF of polymers usually show complex decay dynamics at room temperature that cannot be fitted by sums of exponentials. This is because DF components originate from TADF, not triplet–triplet annihilation. Moreover, the DF of TADF polymers, as with small molecules, exhibits perfect linear dependence with excitation dose. This is because DF originates from a monomolecular process, whereas triplet–triplet annihilation is a bimolecular process[3,25]. In terms of the temperature dependence of TADF polymer emission, the PF components show nearly no variation with temperature because of negligible internal conversion. By contrast, the DF components increase with increasing temperature, indicating definite TADF from RISC, rather than triplet–triplet annihilation. Moreover, the fluorescence decay in the DF region becomes more complex with temperature, accounting for the increasing contribution from long lifetime ^{3}LE phosphorescence and increasing triplet–triplet annihilation. The large proportion of DF is favourable for producing TADF polymeric emitters with relatively high efficiency. However, the DF lifetime of polymers must be rationally

Table 3 | **Summary of photoluminescence and electroluminescence characteristics of representative polymer TADF materials.**

Polymer	λ_{max} (nm)	ΔE_{ST} (eV)	Φ_{PL}/Φ_{DF} (%)	τ_{PF} (ns)/τ_{DF} (μs)	V_{on} (V)	L_{max} (cd m^{-2})	CE (cd A^{-1})	PE (lm W^{-1})	EQE$_{max}$ (%)	CIE (x, y)	Refs
P1	535	0.22	41.0 ± 0.8[a], 43.6 ± 0.9[b]/–	–/–	3.2	>1,000	–	–	10 ± 0.5	(0.32, 0.58)	129
P2	472[a], 508[d]	0.18	28[b], 23[c]/16	13/74	6.0	5,100	24.9	9.0	8.1	(0.28, 0.43)	127
P3	550[a], 540[d]	0.10	26[b], 46[c]/27	24/10	4.3	30,800	31.8	20.3	9.3	(0.38, 0.57)	127
P4	535	–	–/–	–/–		>1,000	10	3.9	11.05	–	130
P5	472[a], 487[d]	0.37	9[a], 9[b], 8[d]/12[b], 6[c]	5.8/0.50	3.0	554	3.6	3.67	1.34	(0.25, 0.47)	128
P6	510[a], 507[d]	0.13	22[a], 40[b], 28[d]/42[b], 14[c]	13.8/0.68	2.6	10,251	41.8	37.1	12.63	(0.30, 0.59)	128
	–	–	–	–	2.5	26,321	48.2	50.1	14.9	(0.34, 0.56)	145
P7	475	0.023	71/50.79	9.44 ± 0.23/296 ± 16	–	–	–	–	–	–	138
P8	535	0.35	–/44.4	–/–	–	>1,000	6.3	2.5	2.3	–	130
	–	–	–	–	5.8	>1,000	61.3	40.1	20.1	(0.36, 0.55)	50
P9	494	–	33.7/1.5[b], 4.5[c]	9.59[b], 8.82[c]/4.06[b], 2.36[c]	3.1	>4,000	10.7	11.2	4.3	(0.24, 0.43)	133
P10	511[b], 500[c]	–	67[b], 74[c]/72	19.5/2.0	7.5	>1,000	38.6	14.3	16.1	(0.22, 0.40)	134
P11	430	0.31	69[b], 71[c]/–	11/50	5.3	899	1.6	0.9	2.0	(0.12, 0.13)	135
P12	402[a], 581[a]/416[d], 567[d]	0.26	99[c]/10.3	25.4/6.2	7.0	15,410	42.4	17.9	19.4	(0.51, 0.47)	131
P13	420[a], 550[a]/531[d]	0.09	89[c]/51	27.9/1.1	2.57	15,456	48.7	50.5	15.5	(0.41, 0.55)	132
	–	–	–	–	2.80	25,864	49.8	49.6	16.0	(0.41, 0.55)	132
P14	489[a]	0.021	60[c], 39[d]/13	24.3/1.2	3.2	6,150	24.8	–	12.1	(0.18, 0.27)	136
P15	369[a], 444[a]	–	9[c], 8[d]/–	15.5/–	5.8	140	0.51	–	0.33	(0.21, 0.20)	136

[a]Measured in solution in air. [b]Measured in solution under N_2. [c]Measured in film under N_2. [d]Measured in film in air. CE, maximum current efficiency; CIE, Commission Internationale de l'Éclairage; EQE$_{max}$, maximum external quantum efficiency; ΔE_{ST}, singlet–triplet energy splitting; L_{max}, maximum luminance; PE, maximum power efficiency; TADF, thermally activated delayed fluorescence; V_{on}, turn-on voltage at 1 cd m^{-2}; Φ_{DF}, delayed fluorescence quantum yield; Φ_{PL}, photoluminescence quantum yield; λ_{max}, wavelength of maximum luminescence; τ_{DF}, delayed fluorescence lifetime; τ_{PF}, prompt fluorescence decay lifetime.

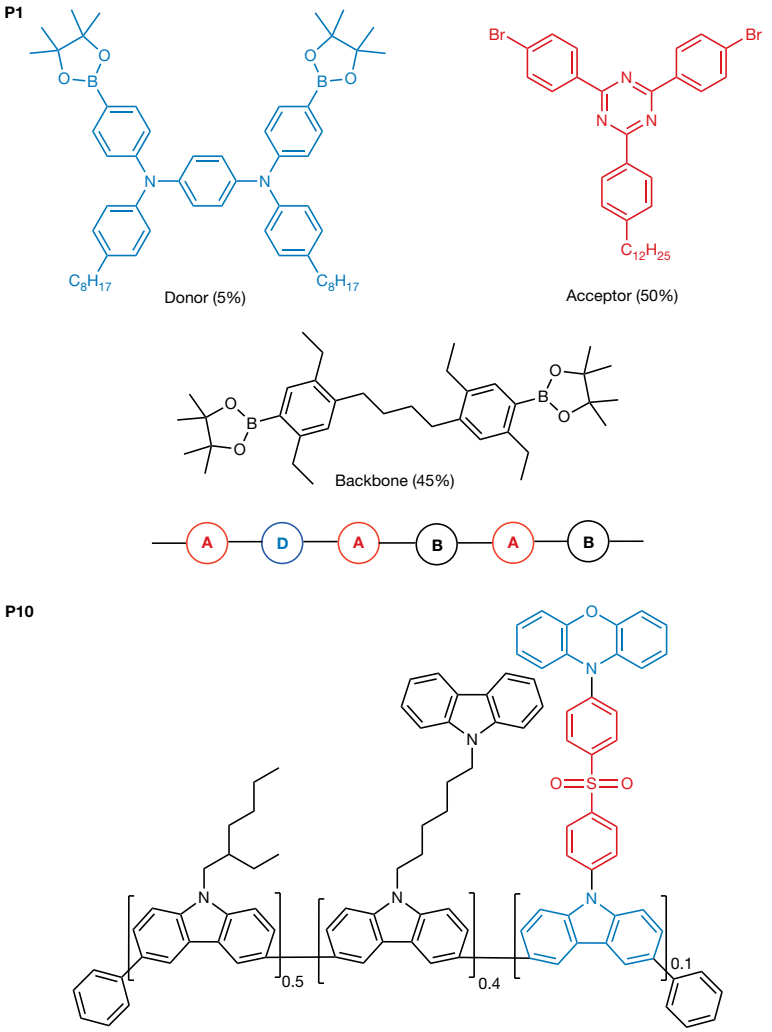

Figure 6 | **Molecular structures of TADF polymers. P1** is a thermally activated delayed fluorescence (TADF) polymer in which the charge transfer emitter is a triazine–amine–triazine unit and the non-conjugated moiety serves as the backbone to isolate the TADF units. **P10** is a typical side-chain polymeric TADF molecule (PCzDP-10) with an asymmetric donor$_1$–acceptor–donor$_2$-type TADF moiety and poly(3,6-carbazole) as the conjugated backbone.

balanced to improve the efficiency. A long lifetime of excitons would increase the nonradiative transitions, resulting in low PLQY and strong efficiency roll-off. For example, pCzBP[127] (**P2**; TABLE 3) displays relatively low PLQY and increased efficiency roll-off owing to the longer TADF lifetime.

PLED fabrication and performance

To date, most TADF polymer LEDs (PLEDs) suffer from unsatisfactory EQEs and appreciable efficiency roll-off compared with small-molecule OLEDs. However, if improvements in these properties can be achieved, the inherent advantages of PLEDs (for example, large-area fabrication with flexible substrates using low-cost solution processing) could be exploited.

Both doped and non-doped emitting layers have been used in solution-processed TADF PLEDs. For a non-doped emitting layer, the presence of a single-component system (as opposed to a host–dopant system) is beneficial for eliminating phase separation and reducing charge trapping and scattering defects[139–143]. For example, PLEDs fabricated using only the TADF polymer (**P1**; TABLE 3) displayed an EQE_{max} of 10% at low current densities[129]. In general, high efficiency roll-off is observed, which is ascribed to triplet quenching[144]. However, extremely low-efficiency roll-off has been achieved by tuning the ratios of donor and acceptor units in a conjugated backbone, thus balancing charge injection and transport[132] (**P13**; TABLE 3). In addition, PLEDs with an in situ thermally crosslinked emitting layer[135] (**P11**; TABLE 3) exhibit an EQE_{max} of 2.0% and small roll-off owing to the short triplet exciton decay lifetime.

In contrast to non-doped emitting layers, a doped emitting layer can overcome the problem of exciton quenching caused by aggregation and unbalanced charge transport. For example, the electroluminescence performance can be improved with TAPC as a host for PAPTC compared with a pure PAPTC emitting layer. The improved efficiency roll-off can be partly ascribed to the formation of an interfacial exciplex host of TAPC/TmPyPB and a further increase in RISC rates of triplets[145] (**P6**; TABLE 3). In another example, a mixed host (TCTA and TAPC) with high T_1 energies was used to fabricate the emitting layer by blending TADF polymer **P2** to improve charge injection and balance, to broaden the recombination zone and to reduce efficiency roll-off. The device structure is shown in FIG. 7a (REFS[144,146,147]). In addition, the blended films have very smooth surface topographies. On the basis of a blended host–guest emitting layer, the assistant dopant DMAC-DP-Cz and mCP host, together with the TADF polymer PCzDP-10 (**P10**; FIG. 6; TABLE 3), were mixed as the light-emitting layer. The resulting PLEDs show remarkably improved performance with an EQE of 16.1% with a 110 nm-thick emitting layer[134]. In these PLEDs, the injected charges are first trapped on the assistant dopant owing to the high HOMO and low LUMO energies of DMAC-DP-Cz; subsequently, the excitons transfer to the singlet and triplet states of the TADF polymer (FIG. 7b).

Future perspectives

The electroluminescent performance of TADF molecules has recently exceeded that of phosphorescent complexes[29,46–48]. In addition, TADF molecules have other advantages for use in OLEDs and solid-state lighting technologies — for example, the use of heavy metals is circumvented, starting materials are of low cost, the chemical structures are versatile and controllable, and the materials are easily prepared. However, the intricacies of the TADF mechanism and the development of higher-efficiency devices remain to be fully explored and unravelled.

In terms of designing TADF molecules, new donors and acceptors, as well as their bridging linkers, are needed to refine our understanding of the fundamental photophysics of small molecules, including the roles of conformational effects. Optimization of the molecular geometry will lead to smaller ΔE_{ST} values, shorter DF lifetimes, higher PLQY and a narrower full width at half

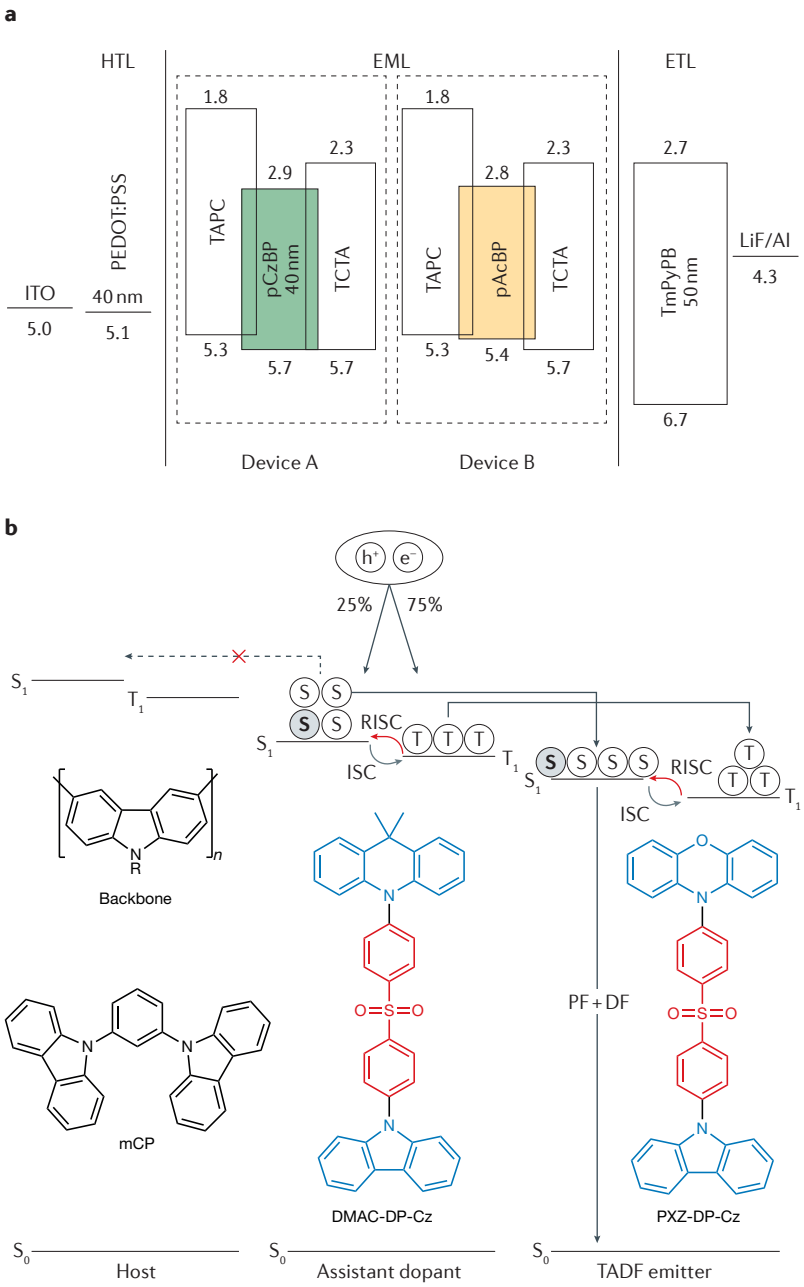

Figure 7 | **Device structure of TADF polymer OLEDs. a** | Energy-level diagram and device structures of pCzBP-based and pAcBP-based organic light-emitting diodes (OLEDs): ITO/PEDOT:PSS (40 nm)/10 wt% polymer:TCTA:TAPC blend (40 nm)/TmPyPB (50 nm)/LiF (0.8 nm)/Al (80 nm), with pCzBP as the emitter in Device A and pAcBP as the emitter in Device B[127]. **b** | The proposed energy-transfer process in the emitting layers of assistant dopant-based TADF polymer OLEDs. In the emitting layer, the injected carriers are transported on the polymer backbone and the mCP host. The carriers are eventually trapped on the assistant dopant as a consequence of the favourable alignment of the highest occupied molecular orbital (HOMO) and lowest unoccupied molecular orbital (LUMO) levels of the dopant compared with those of the host materials. The singlet and triplet excitons in the thermally activated delayed fluorescence (TADF) assistant dopant of DMAC-DP-Cz are transferred into the singlet and triplet states of the side-chain TADF units in the polymer. The triplet excitons of DMAC-DP-Cz convert into singlet states by a reverse intersystem crossing (RISC) process. The same process occurs for side-chain TADF units in the polymer[134]. DF, delayed fluorescence; EMLs, emitting layers; ETL, electron-transport layer; HTL, hole-transport layer; ISC, intersystem crossing; PF, prompt fluorescence. Panel **a** is adapted with permission from REF.[127], Wiley-VCH. Panel **b** is adapted with permission from REF.[134], Wiley-VCH.

maximum in the emission spectra. In terms of dendrimers, the effect of different dendrons on the same TADF core should be studied. Furthermore, hyperbranched polymers incorporating donor–acceptor structural units should be developed owing to their good solubility and low viscosity, which could improve processability in comparison with straight chain TADF polymers[148].

For TADF polymers, an important research focus is the design of copolymers and homopolymers for white-light emission or emission of a specific colour. In TADF copolymers, monomers without TADF characteristics are generally copolymerized with TADF monomers to separate TADF units and thus prevent fluorescence quenching. Therefore, in addition to the choice of TADF monomers, the type of spacers, such as electron transporting or hole transporting, should be carefully selected to optimize the TADF characteristics of the copolymers[149]. Developing high-purity polymers (that is, polymers with narrow polydispersity and negligible defects) is still demanding. In this situation, the exact relationship between the TADF characteristics, device performance and polymer structures can potentially be established. Additionally, comparing the optoelectronic properties (ΔE_{ST}, PLQY and τ_{DF}) of dendrimers or polymers with those of the corresponding monomers may help in the design of high-efficiency TADF polymers.

Low-cost solution processing is suitable for large-area production and makes the practical application of OLEDs feasible. For this processing method, good solubility of small-molecule and macromolecular TADF materials in common solvents is required. However, at present, most TADF materials for the active layers of OLEDs are prepared by thermal evaporation in vacuum owing to their limited solubility. However, in some cases, alkyl or alkoxyl substitutes, which serve to enhance solubility, can reduce or even prevent TADF[150]; thus, the emission characteristics and solubility must be balanced with caution.

Recently, aggregation-induced emission or aggregation-enhanced emission combined with TADF has improved the PLQY in solid films[88,151] and enabled variable emission colours in water–solvent solutions[152]. Designing TADF molecules with aggregation-induced emission or aggregation-enhanced emission properties is promising for applications such as hole-transport or electron-transport materials, exciton-blocking materials and structurally integrated OLED-based luminescent chemical and biological sensors[153].

For macromolecular TADF materials, photophysical mechanisms are very complex and require further study. For example, the effect of systematic changes in the conformation of molecular chains and end-group structure on the properties of TADF polymers is an unexplored topic. In addition to the molecular compositions of TADF polymers, the effect of the condensed state of polymer films on the TADF characteristics and performance also needs to be clarified. The stacking of the polymer chains, the crystallization of the polymers and the orientation of the polymer chains in the thin films may influence the TADF characteristics and device performance and may improve the efficiency of OLEDs[129,154,155].

In-depth computational predictions and optimization of TADF materials are expected to contribute significantly to the future development of the field. For example, quantum chemical calculations could screen out low-efficiency molecules and allow experimental effort to focus on the more promising molecular candidates. For quantum chemical calculations, time-dependent density functional theory is commonly used to theoretically predict the singlet and triplet transition energies of TADF molecules[20,154]. Specifically, application of the descriptor-based optimal Hartree–Fock percentage method and the optimally tuned range-separated functional is a promising approach for the more precise prediction of transition energies of TADF systems[156–158].

Finally, from the viewpoint of electroluminescent devices, high performance needs to be combined with low efficiency roll-off, good colour stability and long device lifetimes[159,160]. These factors will determine the commercial future of TADF materials. Realizing high-performance solution-processable non-doped devices remains a challenge. In this regard, TADF dendrimers and polymers with blue, red and white emission colours are particularly desirable targets. Energy transfer using TADF assistant dopants combined with a conventional fluorescent emitter dopant (in small-molecule and polymer devices) is an emergent strategy to improve OLED performance[161]. To date, traditional device structures for fluorescent and phosphorescent emitters have generally been used in TADF OLEDs and to increase the performance of TADF OLEDs, but alternative device structures should be considered. These device architectures should be tailored to the molecular features of TADF materials to improve the overall performances of OLEDs. Specifically, there is a need to reduce the concentration quenching effect caused by triplet excitons. As an alternative to host–guest emitting layers, quantum well structures, which can effectively confine the charge carriers and excitons, afford high-efficiency devices with low efficiency roll-off[162]. Alternatively, p–n heterojunction device configurations can impart extremely low operating voltages and high efficiencies to OLEDs[123].

1. Tang, C. W. & VanSlyke, S. A. Organic electroluminescent diodes. *Appl. Phys. Lett.* **51**, 913–915 (1987).
This is a seminal paper describing the first OLEDs with a double-layer thin-film structure operating at a voltage below 10V.
2. Friend, R. H. et al. Electroluminescence in conjugated polymers. *Nature* **397**, 121–128 (1999).
3. Adachi, C., Baldo, M. A., Thompson, M. E. & Forrest, S. R. Nearly 100% internal phosphorescence efficiency in an organic light-emitting device. *J. Appl. Phys.* **90**, 5048–5051 (2001).
4. Lee, C. W. & Lee, J. Y. Above 30% external quantum efficiency in blue phosphorescent organic light-emitting diodes using pyrido[2,3-*b*]indole derivatives as host materials. *Adv. Mater.* **25**, 5450–5454 (2013).
5. Baldo, M. A. et al. Highly efficient phosphorescent emission from organic electroluminescent devices. *Nature* **395**, 151–154 (1998).
6. Uoyama, H., Goushi, K., Shizu, K., Nomura, H. & Adachi, C. Highly efficient organic light-emitting diodes from delayed fluorescence. *Nature* **492**, 234–238 (2012).
This is a representative paper on TADF small molecules achieving nearly 100% IQE and nearly 20% electroluminescence efficiency.
7. Goushi, K., Yoshida, K., Sato, K. & Adachi, C. Organic light-emitting diodes employing efficient reverse intersystem crossing for triplet-to-singlet state conversion. *Nat. Photon.* **6**, 253–258 (2012).
8. Zhang, Q. et al. Design of efficient thermally activated delayed fluorescence materials for pure blue organic light emitting diodes. *J. Am. Chem. Soc.* **134**, 14706–14709 (2012).
9. Hedley, G. J., Ruseckas, A. & Samuel, I. D. W. Ultrafast luminescence in $Ir(ppy)_3$. *Chem. Phys. Lett.* **450**, 292–296 (2008).
10. Lawetz, V., Siebrand, W. & Orlandi, G. J. Theory of intersystem crossing in aromatic hydrocarbons. *Chem. Phys.* **56**, 4058–4072 (1972).
11. Robinson, G. W. & Frosch, R. P. Electronic excitation transfer and relaxation. *J. Chem. Phys.* **38**, 1187–1203 (1963).
12. Kono, H., Lin, S. H. & Schlag, E. W. On the role of low-frequency modes in the energy or temperature dependence of intersystem crossing. *Chem. Phys. Lett.* **145**, 280–285 (1988).
13. Fukumura, H., Kikuchi, K., Koike, K. & Kokubun, H. Temperature effect on inverse intersystem crossing of anthracenes. *J. Photochem. Photobiol. A Chem.* **42**, 283–291 (1988).
14. Tanaka, F., Okamoto, M. & Hirayama, S. Pressure and temperature dependences of the rate constant for S_1-T_2 intersystem crossing of anthracene compounds in solution. *J. Phys. Chem.* **99**, 525–530 (1995).
15. Ziegler, T., Rauk, A. & Baerends, E. J. On the calculation of multiplet energies by the Hartree-Fock-Slater method. *Theor. Chim. Acta* **43**, 261–271 (1977).
16. El-Sayed, M. A. Spin-orbit coupling and the radiationless processes in nitrogen heterocyclics. *J. Chem. Phys.* **38**, 2834–2838 (1963).
17. Czerwieniec, R., Leitl, M. J., Homeier, H. H. H. & Yersin, H. Cu(I) complexes — thermally activated delayed fluorescence. Photophysical approach and material design. *Coord. Chem. Rev.* **325**, 2–28 (2016).
18. Pan, Y. et al. High yields of singlet excitons in organic electroluminescence through two paths of cold and hot excitons. *Adv. Opt. Mater.* **2**, 510–515 (2014).
19. Wang, S. et al. Highly efficient near-infrared delayed fluorescence organic light emitting diodes using a phenanthrene-based charge-transfer compound. *Angew. Chem. Int. Ed.* **54**, 13068–13072 (2015).
20. Samanta, P. K., Kim, D., Coropceanu, V. & Brédas, J.-L. Up-conversion intersystem crossing rates in organic emitters for thermally activated delayed fluorescence: impact of the nature of singlet versus triplet excited states. *J. Am. Chem. Soc.* **139**, 4042–4051 (2017).
21. Dias, F. B. et al. Triplet harvesting with 100% efficiency by way of thermally activated delayed fluorescence in charge transfer OLED emitters. *Adv. Mater.* **25**, 3707–3714 (2013).
This study provides a systematic discussion of the factors affecting the efficiency of TADF small-molecule OLEDs, in which detailed molecular structure–photophysics relationships are revealed.
22. Malrieu, J.-P. & Pullman, B. Configuration spatiale et propriétés électroniques du noyau d'isoalloxazine. *Theor. Chim. Acta* **2**, 302–314 (1964).
23. Aizenshtat, Z., Klein, E., Weiler-Feilchenfeld, H. & Bergmann, E. D. Conformational studies on xanthene, thioxanthene and acridan. *Isr. J. Chem.* **10**, 753–763 (1972).
24. Zhang, Q. et al. Anthraquinone-based intramolecular charge-transfer compounds: computational molecular design, thermally activated delayed fluorescence, and highly efficient red electroluminescence. *J. Am. Chem. Soc.* **136**, 18070–18081 (2014).
25. Endo, A. et al. Efficient up-conversion of triplet excitons into a singlet state and its application for organic light emitting diodes. *Appl. Phys. Lett.* **98**, 083302 (2011).
This study was the starting point for purely organic TADF emitters with a very small singlet–triplet gap.
26. Zhang, Q. et al. Efficient blue organic light-emitting diodes employing thermally activated delayed fluorescence. *Nat. Photon.* **8**, 326–332 (2014).
27. Lee, D. R. et al. Design strategy for 25% external quantum efficiency in green and blue thermally activated delayed fluorescent devices. *Adv. Mater.* **27**, 5861–5867 (2015).
28. Li, J. et al. Highly efficient organic light-emitting diode based on a hidden thermally activated delayed fluorescence channel in a heptazine derivative. *Adv. Mater.* **25**, 3319–3323 (2013).
29. Lin, T. A. et al. Sky-blue organic light emitting diode with 37% external quantum efficiency using thermally activated delayed fluorescence from spiroacridine-triazine hybrid. *Adv. Mater.* **28**, 6976–6983 (2016).
This study demonstrates that the maximum EQE of TADF small-molecule OLEDs fabricated by vacuum deposition reaches 36.7%.
30. Tsai, W. L. et al. A versatile thermally activated delayed fluorescence emitter for both highly efficient doped and non-doped organic light emitting devices. *Chem. Commun.* **51**, 13662–13665 (2015).
31. Im, Y. et al. Molecular design strategy of organic thermally activated delayed fluorescence emitters. *Chem. Mater.* **29**, 1946–1963 (2017).
32. Hatakeyama, T. et al. Ultrapure blue thermally activated delayed fluorescence molecules: efficient HOMO-LUMO separation by the multiple resonance effect. *Adv. Mater.* **28**, 2777–2781 (2016).
33. Cho, Y. J., Jeon, S. K., Lee, S.-S., Yu, E. & Lee, J. Y. Donor interlocked molecular design for fluorescence-like narrow emission in deep blue thermally activated delayed fluorescent emitters. *Chem. Mater.* **28**, 5400–5405 (2016).
34. Lee, I. & Lee, J. Y. Molecular design of deep blue fluorescent emitters with 20% external quantum efficiency and narrow emission spectrum. *Org. Electron.* **29**, 160–164 (2016).
In this study, deep-blue TADF OLEDs are reported based on the rational design of the emitter molecule and host material.
35. Cui, L.-S. et al. Long-lived efficient delayed fluorescence organic light-emitting diodes using n-type hosts. *Nat. Commun.* **8**, 2250 (2017).
36. Kim, H. M., Choi, J. M. & Lee, J. Y. Blue thermally activated delayed fluorescent emitters having a bicarbazole donor moiety. *RSC Adv.* **6**, 64133–64139 (2016).
37. Lee, D. R., Choi, J. M., Lee, C. W. & Lee, J. Y. Ideal molecular design of blue thermally activated delayed fluorescent emitter for high efficiency, small singlet-triplet energy splitting, low efficiency roll-off, and long lifetime. *ACS Appl. Mater. Interfaces* **8**, 23190–23196 (2016).
38. Parker, C. A. & Hatchard, C. G. Triplet-singlet emission in fluid solutions: phosphorescence of eosin. *Trans. Faraday Soc.* **57**, 1894–1904 (1961).

39. Endo, A. et al. Thermally activated delayed fluorescence from Sn^{4+}-porphyrin complexes and their application to organic light emitting diodes — a novel mechanism for electroluminescence. *Adv. Mater.* **21**, 4802–4806 (2009).
40. Chen, X.-L. et al. Rational design of strongly blue-emitting cuprous complexes with thermally activated delayed fluorescence and application in solution-processed OLEDs. *Chem. Mater.* **25**, 3910–3920 (2013).
41. Liang, D. et al. Highly efficient cuprous complexes with thermally activated delayed fluorescence for solution-processed organic light-emitting devices. *Inorg. Chem.* **55**, 7467–7475 (2016).
42. Hofbeck, T. Monkowius, U. & Yersin, H. Highly efficient luminescence of Cu(I) compounds: thermally activated delayed fluorescence combined with short-lived phosphorescence. *J. Am. Chem. Soc.* **137**, 399–404 (2015).
43. Volz, D. et al. Bridging the efficiency gap: fully bridged dinuclear Cu(I)-complexes for singlet harvesting in high-efficiency OLEDs. *Adv. Mater.* **27**, 2538–2543 (2015).
44. Mehes, G., Nomura, H., Zhang, Q., Nakagawa, T. & Adachi, C. Enhanced electroluminescence efficiency in a spiro-acridine derivative through thermally activated delayed fluorescence. *Angew. Chem. Int. Ed.* **51**, 11311–11315 (2012).
45. Kim, B. S. & Lee, J. Y. Engineering of mixed host for high external quantum efficiency above 25% in green thermally activated delayed fluorescence device. *Adv. Funct. Mater.* **24**, 3970–3977 (2014).
46. Lee, D. R. et al. Above 30% external quantum efficiency in green delayed fluorescent organic light-emitting diodes. *ACS Appl. Mater. Interfaces* **7**, 9625–9629 (2015).
47. Sun, J. W. et al. A fluorescent organic light-emitting diode with 30% external quantum efficiency. *Adv. Mater.* **26**, 5684–5688 (2014).
48. Zeng, W. et al. Achieving nearly 30% external quantum efficiency for orange-red organic light emitting diodes by employing thermally activated delayed fluorescence emitters composed of 1, 8-naphthalimide-acridine hybrids. *Adv. Mater.* **30**, 1704961 (2017).
49. Li, Y., Xie, G., Gong, S., Wu, K. & Yang, C. Dendronized delayed fluorescence emitters for non-doped, solution-processed organic light-emitting diodes with high efficiency and low efficiency roll-off simultaneously: two parallel emissive channels. *Chem. Sci.* **7**, 5441–5447 (2016).
50. Ren, Z. et al. Pendant homopolymer and copolymers as solution-processable thermally activated delayed fluorescence materials for organic light-emitting diodes. *Macromolecules* **49**, 5452–5460 (2016).
In this study, the maximum EQE of a polymer OLED reaches 20% using the strategy of pendant TADF moieties in the side chain of a polymer.
51. Lee, S. Y., Yasuda, T., Yang, Y. S., Zhang, Q. & Adachi, C. Luminous butterflies: efficient exciton harvesting by benzophenone derivatives for full-color delayed fluorescence OLEDs. *Angew. Chem. Inter. Ed.* **53**, 6402–6406 (2014).
52. Ban, X. et al. Design of encapsulated hosts and guests for highly efficient blue and green thermally activated delayed fluorescence OLEDs based on a solution-process. *Chem. Commun.* **53**, 11834–11837 (2017).
53. Tsang, D. P. K., Matsushima, T. & Adachi, C. Operational stability enhancement in organic light-emitting diodes with ultrathin Liq interlayers. *Sci. Rep.* **6**, 22463 (2016).
54. Cho, Y. J., Yook, K. S. & Lee, J. Y. A universal host material for high external quantum efficiency close to 25% and long lifetime in green fluorescent and phosphorescent OLEDs. *Adv. Mater.* **26**, 4050–4055 (2014).
55. Wong, M. Y. & Zysman-Colman, E. Purely organic thermally activated delayed fluorescence materials for organic light-emitting diodes. *Adv. Mater.* **29**, 1605444 (2017).
56. Ritchie, J., Crayston, J. A., Markham, J. P. & Samuel, I. D. Effect of meta-linkages on the photoluminescence and electroluminescence properties of light-emitting polyfluorene alternating copolymers. *J. Mater. Chem.* **16**, 1651–1656 (2006).
57. Ahn, T., Jang, M. S., Shim, H. K., Hwang, D. H. & Zyung, T. Blue electroluminescent polymers: control of conjugation length by kink linkages and substituents in the poly (*p*-phenylenevinylene)-related copolymers. *Macromolecules* **32**, 3279–3285 (1999).
58. Tanaka, H., Shizu, K., Miyazaki, H. & Adachi, C. Efficient green thermally activated delayed fluorescence (TADF) from a phenoxazine-triphenyltriazine (PXZ-TRZ) derivative. *Chem. Commun.* **48**, 11392–11394 (2012).
59. Kaji, H. et al. Purely organic electroluminescent material realizing 100% conversion from electricity to light. *Nat. Commun.* **6**, 8476 (2015).
60. Shizu, K. et al. Highly efficient blue electroluminescence using delayed-fluorescence emitters with large overlap density between luminescent and ground states. *J. Phys. Chem. C* **119**, 26283–26289 (2015).
61. Serevicius, T. et al. Enhanced electroluminescence based on thermally activated delayed fluorescence from a carbazole-triazine derivative. *Phys. Chem. Chem. Phys.* **15**, 15850–15855 (2013).
62. Hirata, S. et al. Highly efficient blue electroluminescence based on thermally activated delayed fluorescence. *Nat. Mater.* **14**, 330–336 (2015).
This report reveals the compatibility between low ΔE_{st} and high PLQY and produces a blue emitter with near 100% internal electroluminescence quantum yield.
63. Park, I. S., Lee, S. Y., Adachi, C. & Yasuda, T. Full-color delayed fluorescence materials based on wedge-shaped phthalonitriles and dicyanopyrazines: systematic design, tunable photophysical properties, and OLED performance. *Adv. Funct. Mater.* **26**, 1813–1821 (2016).
64. Liu, M. et al. Blue thermally activated delayed fluorescence materials based on bis(phenylsulfonyl) benzene derivatives. *Chem. Commun.* **51**, 16353–16356 (2015).
65. Wang, Z. et al. Structure-performance investigation of thioxanthone derivatives for developing color tunable highly efficient thermally activated delayed fluorescence emitters. *ACS Appl. Mater. Interfaces* **8**, 8627–8636 (2016).
66. Kawasumi, K. et al. Thermally activated delayed fluorescence materials based on homoconjugation effect of donor-acceptor triptycenes. *J. Am. Chem. Soc.* **137**, 11908–11911 (2015).
67. Nakagawa, T., Ku, S. Y., Wong, K. T. & Adachi, C. Electroluminescence based on thermally activated delayed fluorescence generated by a spirobifluorene donor-acceptor structure. *Chem. Commun.* **48**, 9580–9582 (2012).
68. Chen, X.-K. et al. A new design strategy for efficient thermally activated delayed fluorescence organic emitters: from twisted to planar structures. *Adv. Mater.* **29**, 1702767 (2017).
69. Nishimoto, T., Yasuda, T., Lee, S. Y., Kondo, R. & Adachi, C. A six-carbazole-decorated cyclophosphazene as a host with high triplet energy to realize efficient delayed-fluorescence OLEDs. *Mater. Horiz.* **1**, 264–269 (2014).
70. Lin, M.-S. et al. Incorporation of a CN group into mCP: a new bipolar host material for highly efficient blue and white electrophosphorescent devices. *J. Mater. Chem.* **22**, 16114–16120 (2012).
71. Cho, Y. J., Yook, K. S. & Lee, J. Y. High efficiency in a solution-processed thermally activated delayed-fluorescence device using a delayed-fluorescence emitting material with improved solubility. *Adv. Mater.* **26**, 6642–6646 (2014).
This paper pioneers solution-processed TADF small-molecule emitting materials: the corresponding OLED device exhibits a high electro-luminescence efficiency of 18.3%.
72. Tsai, Y. S., Hong, L. A., Juang, F. S. & Chen, C. Y. Blue and white phosphorescent organic light emitting diode performance improvement by confining electrons and holes inside double emitting layers. *J. Lumin.* **153**, 312–316 (2014).
73. Senes, A. et al. Increasing the horizontal orientation of transition dipole moments in solution processed small molecular emitters. *J. Mater. Chem. C* **5**, 6555–6562 (2017).
74. Kim, B. S. & Lee, J. Y. Phosphine oxide type bipolar host material for high quantum efficiency in thermally activated delayed fluorescent device. *ACS Appl. Mater. Interfaces* **6**, 8396–8400 (2014).
75. Seino, Y., Inomata, S., Sasabe, H., Pu, Y. J. & Kido, J. High-performance green OLEDs using thermally activated delayed fluorescence with a power efficiency of over 100lm W^{-1}. *Adv. Mater.* **28**, 2638–2643 (2016).
76. Gaj, M. P., Fuentes-Hernandez, C., Zhang, Y., Marder, S. R. & Kippelen, B. Highly efficient organic light-emitting diodes from thermally activated delayed fluorescence using a sulfone–carbazole host material. *Org. Electron.* **16**, 109–112 (2015).
77. Fan, C. et al. Dibenzothiophene-based phosphine oxide host and electron-transporting materials for efficient blue thermally activated delayed fluorescence diodes through compatibility optimization. *Chem. Mater.* **27**, 5131–5140 (2015).
78. Ding, D., Zhang, Z., Wei, Y., Yan, P. & Xu, H. Spatially optimized quaternary phosphine oxide host materials for high-efficiency blue phosphorescence and thermally activated delayed fluorescence organic light-emitting diodes. *J. Mater. Chem. C* **3**, 11385–11396 (2015).
79. Zhang, J. et al. Multiphosphine-oxide hosts for ultralow-voltage-driven true-blue thermally activated delayed fluorescence diodes with external quantum efficiency beyond 20%. *Adv. Mater.* **28**, 479–485 (2016).
80. Dos Santos, P. et al. Using guest-host interactions to optimize the efficiency of TADF OLEDs. *J. Phys. Chem. Lett.* **7**, 3341–3346 (2016).
81. Nishide, J., Nakanotani, H., Hiraga, Y. & Adachi, C. High-efficiency white organic light-emitting diodes using thermally activated delayed fluorescence. *Appl. Phys. Lett.* **104**, 233304 (2014).
82. Zhang, D., Duan, L., Li, Y., Zhang, D. & Qiu, Y. Highly efficient and color-stable hybrid warm white organic light-emitting diodes using a blue material with thermally activated delayed fluorescence. *J. Mater. Chem. C* **2**, 8191–8197 (2014).
83. Li, X. L. et al. High-efficiency WOLEDs with high color-rendering index based on a chromaticity-adjustable yellow thermally activated delayed fluorescence emitter. *Adv. Mater.* **28**, 4614–4619 (2016).
84. Kim, S.-Y. et al. Organic light-emitting diodes with 30% external quantum efficiency based on a horizontally oriented emitter. *Adv. Funct. Mater.* **23**, 3896–3900 (2013).
85. Nowy, S., Krummacher, B. C., Frischeisen, J., Reinke, N. A. & Brütting, W. Light extraction and optical loss mechanisms in organic light-emitting diodes: Influence of the emitter quantum efficiency. *J. Appl. Phys.* **104**, 123109 (2008).
86. Mayr, C. et al. Efficiency enhancement of organic light-emitting diodes incorporating a highly oriented thermally activated delayed fluorescence emitter. *Adv. Funct. Mater.* **24**, 5232–5239 (2014).
87. Zhang, Q. et al. Nearly 100% internal quantum efficiency in undoped electroluminescent devices employing pure organic emitters. *Adv. Mater.* **27**, 2096–2100 (2015).
88. Guo, J. et al. Achieving high-performance nondoped OLEDs with extremely small efficiency roll-off by combining aggregation-induced emission and thermally activated delayed fluorescence. *Adv. Funct. Mater.* **27**, 1606458 (2017).
89. Huang, J. et al. Highly efficient nondoped OLEDs with negligible efficiency roll-off fabricated from aggregation-induced delayed fluorescence luminogens. *Angew. Chem. Int. Ed.* **129**, 13151–13156 (2017).
90. Goushi, K. & Adachi, C. Efficient organic light-emitting diodes through up-conversion from triplet to singlet excited states of exciplexes. *Appl. Phys. Lett.* **101**, 023306 (2012).
91. Liu, X. K. et al. Prediction and design of efficient exciplex emitters for high-efficiency, thermally activated delayed-fluorescence organic light-emitting diodes. *Adv. Mater.* **27**, 2378–2383 (2015).
92. Liu, W. et al. Novel strategy to develop exciplex emitters for high-performance OLEDs by employing thermally activated delayed fluorescence materials. *Adv. Funct. Mater.* **26**, 2002–2008 (2016).
93. Duan, L. et al. Solution processable small molecules for organic light-emitting diodes. *J. Mater. Chem.* **20**, 6392–6407 (2010).
94. Cho, Y. J., Chin, B. D., Jeon, S. K. & Lee, J. Y. 20% external quantum efficiency in solution-processed blue thermally activated delayed fluorescent devices. *Adv. Funct. Mater.* **25**, 6786–6792 (2015).
95. Mei, L. et al. The inductive-effect of electron withdrawing trifluoromethyl for thermally activated delayed fluorescence: tunable emission from *tetra*- to *penta*-carbazole in solution processed blue OLEDs. *Chem. Commun.* **51**, 13024–13027 (2015).

96. Chen, P. et al. Delayed fluorescence in a solution-processable pure red molecular organic emitter based on dithienylbenzothiadiazole: a joint optical, electroluminescence, and magneto electroluminescence study. *ACS Appl. Mater. Interfaces* **7**, 2972–2978 (2015).
97. Wada, Y. et al. Highly efficient electroluminescence from a solution-processable thermally activated delayed fluorescence emitter. *Appl. Phys. Lett.* **107**, 183303 (2015).
98. Xie, G. et al. Evaporation- and solution-process-feasible highly efficient thianthrene-9,9′,10,10′-tetraoxide-based thermally activated delayed fluorescence emitters with reduced efficiency roll-off. *Adv. Mater.* **28**, 181–187 (2016).
99. Schmidbauer, S., Hohenleutner, A. & König, B. Chemical degradation in organic light-emitting devices: mechanisms and implications for the design of new materials. *Adv. Mater.* **25**, 2114–2129 (2013).
100. Cui, L. S. et al. Pure hydrocarbon hosts for ≈100% exciton harvesting in both phosphorescent and fluorescent light-emitting devices. *Adv. Mater.* **27**, 4213–4217 (2015).
101. Cui, L. S. et al. Controlling synergistic oxidation processes for efficient and stable blue thermally activated delayed fluorescence devices. *Adv. Mater.* **28**, 7620–7625 (2016).
102. Kanibolotsky, A. L., Perepichka, I. F. & Skabara, P. J. Star-shaped π-conjugated oligomers and their applications in organic electronics and photonics. *Chem. Soc. Rev.* **39**, 2695–2728 (2010).
103. Burn, P. L., Lo, S. C. & Samuel, D. W. The development of light-emitting dendrimers for displays. *Adv. Mater.* **19**, 1675–1688 (2007).
104. Albrecht, K., Matsuoka, K., Fujita, K. & Yamamoto, K. Carbazole dendrimers as solution-processable thermally activated delayed-fluorescence materials. *Angew. Chem. Int. Ed.* **54**, 5677–5682 (2015).
In this study, a solution-processed dendrimer TADF emitter is reported with a maximum EQE of 3.4%.
105. Luo, J. et al. Multi-carbazole encapsulation as a simple strategy for the construction of solution-processed, non-doped thermally activated delayed fluorescence emitters. *J. Mater. Chem. C* **4**, 2442–2446 (2016).
106. Albrecht, K. et al. Thermally activated delayed fluorescence OLEDs with fully solution processed organic layers exhibiting nearly 10% external quantum efficiency. *Chem. Commun.* **53**, 2439–2442 (2017).
107. Li, J. et al. Deep-blue thermally activated delayed fluorescence dendrimers with reduced singlet-trip let energy gap for low roll-off non-doped solution-processed organic light-emitting diodes. *Dyes Pigments* **140**, 79–86 (2017).
108. Matsuoka, K., Albrecht, K., Yamamoto, K. & Fujita, K. Mulifunctional dendritic emitter: aggregation-induced emission enhanced, thermally activated delayed fluorescent material for solution-processed multilayered organic light-emitting diodes. *Sci. Rep.* **7**, 41780 (2017).
109. Ban, X. et al. Self-host thermally activated delayed fluorescent dendrimers with flexible chains: an effective strategy for non-doped electroluminescent devices based on solution processing. *J. Mater. Chem. C* **4**, 8810–8816 (2016).
110. Ban, X., Jiang, W., Sun, K., Lin, B. & Sun, Y. Self-host blue dendrimer comprised of thermally activated delayed fluorescence core and bipolar dendrons for efficient solution-processable nondoped electroluminescence. *ACS Appl. Mater. Interfaces* **9**, 7339–7346 (2017).
111. Sun, K. et al. Design strategy of yellow thermally activated delayed fluorescent dendrimers and their highly efficient non-doped solution-processed OLEDs with low driving voltage. *Org. Electron.* **42**, 123–130 (2017).
112. Godumala, M. et al. Novel dendritic large molecules as solution-processable thermally activated delayed fluorescent emitters for simple structured non-doped organic light emitting diodes. *J. Mater. Chem. C* **6**, 1160–1170 (2018).
113. Sun, K. et al. Thermally activated delayed fluorescence dendrimers with exciplex-forming dendrons for low-voltage-driving and power-efficient solution-processed OLEDs. *J. Mater. Chem. C* **6**, 43–49 (2018).
114. Wang, Y. et al. Engineering the interconnecting position of star-shaped donor-pi-acceptor molecules based on triazine, spirofluorene, and triphenylamine moieties for color tuning from deep blue to green. *Chem. Asian J.* **11**, 2555–2563 (2016).
115. Xia, D. et al. Self-host blue-emitting Iridium dendrimer with carbazole dendrons: nondoped phosphorescent organic light-emitting diodes. *Angew. Chem. Int. Ed.* **53**, 1048–1052 (2014).
116. Chen, L. et al. Self-host heteroleptic green iridium dendrimers: achieving efficient non-doped device performance based on a simple molecular structure. *Chem. Commun.* **47**, 9519–9521 (2011).
117. Albrecht, K., Kasai, Y., Kimoto, A. & Yamamoto, K. The synthesis and properties of carbazole-phenylazomethine double layer-type dendrimers. *Macromolecules* **41**, 3793–3800 (2008).
118. Zhao, Z. H. et al. Synthesis and properties of dendritic emitters with a fluorinated starburst oxadiazole core and twisted carbazole dendrons. *Macromolecules* **44**, 1405–1413 (2011).
119. Ding, J. et al. Bifunctional green Iridium dendrimers with a "self-host" feature for highly efficient nondoped electrophosphorescent devices. *Angew. Chem. Int. Ed.* **48**, 6664–6666 (2009).
120. Albrecht, K., Pernites, R., Felipe, M. J., Advincula, R. C. & Yamamoto, K. Patterning carbazole-phenylazomethine dendrimer films. *Macromolecules* **45**, 1288–1295 (2012).
121. Kimoto, A. et al. Novel hole-transport material for efficient polymer light-emitting diodes by photoreaction. *Macromol. Rapid Commun.* **26**, 597–601 (2005).
122. Yook, K. S. & Lee, J. Y. Small molecule host materials for solution processed phosphorescent organic light-emitting diodes. *Adv. Mater.* **26**, 4218–4233 (2014).
123. Chen, D. et al. Fluorescent organic planar p-n heterojunction light-emitting diodes with simplified structure, extremely low driving voltage, and high efficiency. *Adv. Mater.* **28**, 239–244 (2016).
124. Sekine, C., Tsubata, Y., Yamada, T., Kitano, M. & Doi, S. Recent progress of high performance polymer OLED and OPV materials for organic printed electronics. *Sci. Technol. Adv. Mater.* **15**, 34203 (2014).
125. Grimsdale, A. C., Chan, K. L., Martin, R. E., Jokisz, P. G. & Holmes, A. B. Synthesis of light-emitting conjugated polymers for applications in electroluminescent devices. *Chem. Rev.* **109**, 897–1091 (2009).
126. Rothe, C. & Monkman, A. Regarding the origin of the delayed fluorescence of conjugated polymers. *J. Chem. Phys.* **123**, 244904 (2005).
127. Lee, S. Y., Yasuda, T., Komiyama, H., Lee, J. & Adachi, C. Thermally activated delayed fluorescence polymers for efficient solution-processed organic light-emitting diodes. *Adv. Mater.* **28**, 4019–4024 (2016).
128. Zhu, Y. et al. Synthesis and electroluminescence of a conjugated polymer with thermally activated delayed fluorescence. *Macromolecules* **49**, 4373–4377 (2016).
129. Nikolaenko, A. E., Cass, M., Bourcet, F., Mohamad, D. & Roberts, M. Thermally activated delayed fluorescence in polymers: a new route toward highly efficient solution processable OLEDs. *Adv. Mater.* **27**, 7236–7240 (2015).
130. Nobuyasu, R. S. et al. Rational design of TADF polymers using a donor-acceptor monomer with enhanced TADF efficiency induced by the energy alignment of charge transfer and local triplet excited states. *Adv. Opt. Mater.* **4**, 597–607 (2016).
131. Wang, Y. et al. Bright white electroluminescence from a single polymer containing a thermally activated delayed fluorescence unit and a solution-processed orange OLED approaching 20% external quantum efficiency. *J. Mater. Chem. C* **5**, 10715–10720 (2017).
132. Wang, Y. et al. Efficient non-doped yellow OLEDs based on thermally activated delayed fluorescence conjugated polymers with an acridine/carbazole donor backbone and triphenyltriazine acceptor pendant. *J. Mater. Chem. C* **6**, 568–574 (2018).
133. Luo, J., Xie, G., Gong, S., Chen, T. & Yang, C. Creating a thermally activated delayed fluorescence channel in a single polymer system to enhance exciton utilization efficiency for bluish-green electroluminescence. *Chem. Commun.* **52**, 2292–2295 (2016).
134. Xie, G. et al. Inheriting the characteristics of TADF small molecule by side-chain engineering strategy to enable bluish-green polymers with high PLQYs up to 74% and external quantum efficiency over 16% in light-emitting diodes. *Adv. Mater.* **29**, 1604223 (2017).
135. Sun, K. et al. Thermally cross-linkable thermally activated delayed fluorescent materials for efficient blue solution-processed organic light-emitting diodes. *J. Mater. Chem. C* **4**, 8973–8979 (2016).
136. Shao, S. et al. Blue thermally activated delayed fluorescence polymers with nonconjugated backbone and through-space charge transfer effect. *J. Am. Chem. Soc.* **139**, 17739–17742 (2017).
137. Köhler, A. & Beljonne, D. The singlet-triplet exchange energy in conjugated polymers. *Adv. Funct. Mater.* **14**, 11–18 (2004).
138. Wei, Q. et al. Conjugation-induced thermally activated delayed fluorescence (TADF): from conventional non-TADF units to TADF-active polymers. *Adv. Funct. Mater.* **27**, 1605051 (2017).
139. Reineke, S. Organic light-emitting diodes: Phosphorescence meets its match. *Nat. Photon.* **8**, 269–270 (2014).
140. Dias, F. B. Kinetics of thermal-assisted delayed fluorescence in blue organic emitters with large singlet-triplet energy gap. *Phil. Trans. R. Soc. A* **373**, 20140447 (2015).
141. Uchida, M., Adachi, M., Koyama, T. & Taniguchi, Y. Charge carrier trapping effect by luminescent dopant molecules in single-layer organic light emitting diodes. *J. Appl. Phys.* **86**, 1680–1687 (1999).
142. Tsung, K. K. & So, S. K. Carrier trapping and scattering in amorphous organic hole transporter. *Appl. Phys. Lett.* **92**, 103315 (2008).
143. Wang, S. et al. Ultrahigh color-stable, solution-processed, white OLEDs using a dendritic binary host and long-wavelength dopants with different charge trapping depths. *Adv. Opt. Mater.* **3**, 1349–1354 (2015).
144. Zhang, Y. & Forrest, S. R. Triplets contribute to both an increase and loss in fluorescent yield in organic light emitting diodes. *Phys. Rev. Lett.* **108**, 267404 (2012).
145. Lin, X. et al. Highly efficient TADF polymer electroluminescence with reduced efficiency roll-off via interfacial exciplex host strategy. *ACS Appl. Mater. Interfaces* **10**, 47–52 (2018).
146. Murawski, C., Leo, K. & Gather, M. C. Efficiency roll-off in organic light-emitting diodes. *Adv. Mater.* **25**, 6801–6827 (2013).
147. Fu, Q., Chen, J., Shi, C. & Ma, D. Solution-processed small molecules as mixed host for highly efficient blue and white phosphorescent organic light-emitting diodes. *ACS Appl. Mater. Interfaces* **4**, 6579–6586 (2012).
148. Wu, W., Tang, R., Li, Q. & Li, Z. Functional hyperbranched polymers with advanced optical, electrical and magnetic properties. *Chem. Soc. Rev.* **44**, 3997–4022 (2015).
149. Li, C. et al. Thermally activated delayed fluorescence pendant copolymers with electron and hole-transporting spacers. *ACS Appl. Mater. Interfaces* **10**, 5731–5739 (2018).
150. Ward, J. S. et al. The interplay of thermally activated delayed fluorescence (TADF) and room temperature organic phosphorescence in sterically-constrained donor-acceptor charge-transfer molecules. *Chem. Commun.* **52**, 2612–2615 (2016).
151. Furue, R., Nishimoto, T., Park, I. S., Lee, J. & Yasuda, T. Aggregation-induced delayed fluorescence based on donor/acceptor-tethered janus carborane triads: unique photophysical properties of nondoped OLEDs. *Angew. Chem. Int. Ed.* **128**, 7287–7291 (2016).
152. Li, C. et al. Solution-processable thermally activated delayed fluorescence white OLEDs based on dual-emission polymers with tunable emission colors and aggregation-enhanced emission properties. *Adv. Opt. Mater.* **5**, 1700435 (2017).
This report provides a novel route of combining TADF and aggregation-induced emission in a polymeric emitter to enhance the efficiency.
153. Shinar, J. & Shinar, R. Organic light-emitting devices (OLEDs) and OLED-based chemical and biological sensors: an overview. *J. Phys. D Appl. Phys.* **41**, 133001 (2008).
154. Freeman, D. M. E. et al. Synthesis and exciton dynamics of donor-orthogonal acceptor conjugated polymers: reducing the singlet-triplet energy gap. *J. Am. Chem. Soc.* **139**, 11073–11080 (2017).
155. Xie, Y. & Li, Z. Thermally activated delayed fluorescent polymers. *J. Polym. Sci. Part A Polym. Chem.* **55**, 575–584 (2017).

156. Huang, S. et al. Computational prediction for singlet- and triplet-transition energies of charge-transfer compounds. *J. Chem. Theory Comput.* **9**, 3872–3877 (2013).
157. Peng, Q. et al. Theoretical study of conversion and decay processes of excited triplet and singlet states in a thermally activated delayed fluorescence molecule. *J. Phys. Chem. C* **121**, 13448–13456 (2017).
158. Tian, X., Sun, H., Zhang, Q. & Adachi, C. Theoretical predication for transition energies of thermally activated delayed fluorescence molecules. *Chinese Chem. Lett.* **27**, 1445–1452 (2016).
159. Chen, X. K., Zhang, S. F., Fan, J. X. & Ren, A. M. Nature of highly efficient thermally activated delayed fluorescence in organic light-emitting diode emitters: nonadiabatic effect between excited states. *J. Phys. Chem. C* **119**, 9728–9733 (2015).
160. Marian, C. M. Mechanism of the triplet-to-singlet up conversion in the assistant dopant Acrxtn. *J. Phys. Chem. C* **120**, 3715–3721 (2016).
161. Nakanotani, H. et al. High-efficiency organic light-emitting diodes with fluorescent emitters. *Nat. Commun.* **5**, 4016 (2014).
162. Meng, L. et al. Highly efficient nondoped organic light emitting diodes based on thermally activated delayed fluorescence emitter with quantum well structure. *ACS Appl. Mater. Interfaces* **8**, 20955–20961 (2016).

Author contributions
All authors researched data for the article and contributed to the discussion of content, as well as the writing and editing of the article, before submission.

Acknowledgements
The financial support of the National Natural Science Foundations of China under Grant Nos. 51521062 and 21274009 (Z.R. and S.Y.) and the Engineering and Physical Sciences Research Council (EPSRC) Grant No. EL/L02621X/1 (M.R.B.) is gratefully acknowledged.

Competing interests
The authors declare no competing interests.

Publisher's note
Springer Nature remains neutral with regard to jurisdictional claims in published maps and institutional affiliations.